A spin-half system as a working substance of a heat engine: exploring its finite-time thermodynamic quantities

A Dissertation Submitted to the Department of Physics Addis Ababa University in Partial Fulfillment of the Requirements for the Degree Doctor of Philosophy (in Physics)

By

Tolasa Adugna Dima

Advisor

Dr. Mulugeta Bekele (Assoc. Professor),

Addis Ababa University

June 27, 2017

Declaration

I hereby declare that except where specific reference is made to the work of others,the contents of this dissertation are original and have not been submitted in whole or in part for consideration for any other degree or qualification in this, or any other University. This dissertation is the result of my own work and that all sources of material used for the dissertation have been duly acknowledged.

Name: Tolasa Adugna Dima

Signature: _____

Date: _____

This PhD dissertation has been submitted for examination with my approval as university advisor.

Advisor's Name: Dr. Mulugeta Bekele

Signature: _____

Date: _____

Approved by the Examination Committee

	Signature	Date
External Examiner: Prof. Purushotam D. Gujrati	_____	_____
Internal Examiner: Dr. Lemi Demeyu	_____	_____
Thesis Advisor: Dr. Mulugeta Bekele	_____	_____
Chairman: Dr. Deribe Hirpo	_____	_____

This work is dedicated solely to

Hawi B. Mosissa.

Acknowledgements

First and above all, I praise Waaqayyo, the almighty for providing me the opportunity to do this work. Next, my special thank goes to my advisor Dr. Mulugeta Bekele for his unreserved support throughout my study. From his friendly approach and fatherhood advice, I have learned and shared lots of experiences. My sincere thanks also goes to Dr. Lemi Demeyu, course instructor and ex-head of physics Department, AAU, for his encouragement, valuable comments and support during my PhD study. The assistance from the physics Department, AAU, Dr. Belayneh Mesfin (ex-dept head), Dr. Teshome Senbeta(current Dept head), Mrs. Tsilat Adnew (Dept Secretary) have been great. I want to say thank you very much to all. I am also very much thankful to Anley Gesese , a friend of mine and a lab-mate, for his invaluable comments on every contents of the thesis, thank you Anley.

Most of all for my loving, supportive and encouraging person-my wife Hawi Bekele Mosissa whose faithful support throughout my PhD study is so appreciated. Hawi, though, most of the time you have been virtually with me during this hardest time of mine, your motivation and advice are all the time been with me; whatever happened, you live in my heart forever. I want to say, *I Love You, Honeye!*. Aga, my son, also deserve love and appreciation.

My mother-in-law, Showaye G. Bayi, and Mrs. Ayantu Lemi who have paid the most expensive price for my PhD study should also deserve sincere thanks and respect!. This family provided accommodations to me and have been taking care of Aga (my son). Adde Shawayee, fayyaa fi umurii dheeraan siniifan hawwa! I am thankful to Ayantu L., Ulfe, Megersa and Misgana S. for their care to me and Ago; God bless you!!!

I also extend my great thanks and gratitude to my parents for their devotion and support to my entire schooling. In particular, my father Adugna Dima, my mother Gete Korje deserve special thanks. Maatiikoo fayyaa wajjin raagaa! I own heartfelt thanks to my brothers: Edossa A. and his wife Birhane G., Ejeta A. and his wife Sara D., Fikadu Debisa Dima, Gezahegn L. and his his wife Zewditu N., Tadese G. and his wife Bayush G., Dessalegn A. and his wife Asrate M., Bonsa A. and Fikadu Debisa Chalchisa and his wife Alemnesh G. I love you and have great respect to you all because you love me, you encourage me even when I have not been good. God bless you and your family, bros! Ejeta, I am saddened by your current condition! I pray for your immediate reunion with your beloved family.

I am again very much thankful to Mr. Tarekegn Dayo, Mrs. Aberash Kebede and their entire family for their financial and material support from as early as my secondary school to the present. I am also thankful to Mr.Lemessa Asefa, (ex-head Physics Dept, AU) and Mr. Dinberu Faji (head Physics Dept, AU), Ambo University (AU) for their support. I thank the Statistical and Computational Science staff members and postgraduate students. The International Physical Sciences (IPS), Uppsala University, Sweden has provided research facilities to our Computational Lab. and hence it is gratefully acknowledged.

Tolasa Adugna

Contents

Abstract

Three different model heat engines, two of which operate between two reservoirs at inverse positive absolute temperatures and a third one that operates between two inverse negative absolute temperatures are investigated. As a working substance of the engines, a system of two-level spin-half particles, in the thermodynamic limit, subjected to a time-dependent external magnetic field, is used. We investigate the heat engines under two schemes: the quasistatic and finite-time thermodynamic processes.

In the quasistatic process the system and the reservoirs essentially remain in thermal equilibrium and exchange energy in the form of heat and work. As they link the isothermal processes, adiabatic changes are also basic components of the quasistatic processes. After setting the models, the expressions for net work done, net heat absorbed and efficiency of each model are analytically derive. For parameter values of energy level spacing, occupation probability in the excited state and inverse temperature, the efficiencies coincide with the Carnot efficiency of each model.

In the finite-time process, the expressions for net work done, power and efficiency of the heat engines are derived. In all the three models, power versus period (τ) initially ($\tau \leq \tau_{mp}$ -period at the maximum power) shows a rapid increase with period; then it shows a maximum value at mp before it decrease as period becomes longer and longer. In the very long period limit, finite-time quantities including power, approach to their corresponding quasistatic values.

Employing a unified criterion for energy converters, the model engines are effectively optimized and found to yield optimum finite-time quantities. Efficiency-wise optimized efficiencies are found to be better than efficiencies at maximum power; however, power-

wise, the optimized power is smaller than its maximum power. The figure of merit of model I, ψ_I, plotted against the quaistaitic efficiency, increases from its 1.12 to about 1.3, as its quasistatic efficiency increases from zero to the maximum possible value. So, in the entire range of η_C , optimum working condition is an advantage for the model. However, the figure of merit of model III, ψ_{III} , generally decreases from its peak value of 1.89 with an increase in η_C . Only in the small η_C 0.2 values, the optimum working condition is preferred to the maximum power working condition. Else where, the maximum working condition is better than the optimum working condition for the model. In model II, the figure of merits, ψ_{II}, slightly decreases from its value of about 1.15 to 1.1 as at η_C increases from zero to 0.57.

List of Figures

Chapter 1

Introduction

1.1 Localized spin system in an external magnetic field

Spin is an intrinsic form of angular momentum carried by elementary particles. Since the components of a spin-half particle subjected to an external magnetic field can have two possible discrete values, it forms a two level state. As their magnetic moment prefers to line up either parallel or anti parallel with the field, these two states are of different energy values. The energy of a spin-half particle with magnetic moment $\boldsymbol{\mu}$ in an external field $\mathbf{B}$ is $E = -\boldsymbol{\mu}.\mathbf{B}$: when its magnetic moment is aligned **a**nti **p**arallel to the field, its energy is $E_{\mathbf{ap}} = \mu B$. When it is aligned **pa**rallel to the field, however, its energy is $E_{\mathbf{pa}} = -\mu B$. Then, the magnitude of the energy difference, Δ, between the two level states is

$$\Delta = 2\mu B. \tag{1.1}$$

For a given magnetic moment μ, the energy level spacing Δ depends on the external magnetic field in which the spin-half particles immersed.

Fig.1.1 depicts the two energy levels of a single spin-half particle in an external magnetic field. When the spin-half particle is aligned opposite to the external field, it is at higher energy (in the excited state) whereas when its is aligned in the direction parallel to the external field, it is at the lower energy (in the ground state).

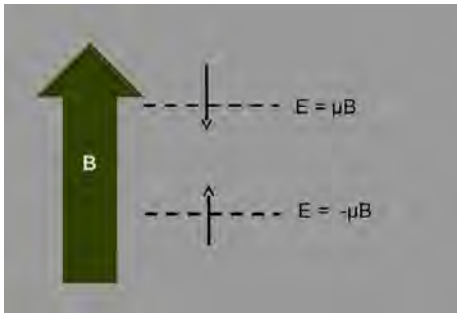

Figure 1.1: A spin-half particle in an external magnetic field **B**. Downward arrow indicates the magnetic moment of spin-half particle aligned anti parallel to the filed (excited state) whereas upward arrow indicates when the magnetic moment of the spin-half particle is aligned parallel to the field (ground state). The bold upward arrow represents the external magnetic field.

Our interest is not in a one particle system; rather, it is in a large number of localized system of spin-half particles in the thermodynamic limit in which the interaction between each spin is assumed to be negligible. In such assembly of spins, the average distance between the particles is assumed to be large enough that the magnetic field produced by one at the position of its nearest neighbor is negligible. Moreover, the spins are assumed to be localized in the sense that each particle is fixed in position like atoms in a solid. This simplifies our system in two ways: firstly, each position of the particle can easily be labeled by assigning a set of numbers to identify each as distinguishable entities. Secondly, motional and other forms of energy associated with spin-half particles can be ignored so that the total energy of the system is due to the interaction of the external field with each spin. The energy, E, of N identical spin-half particles each with the same magnetic moment $\boldsymbol{\mu}$ in an external magnetic field, **B**, is then

$$E = -(N_1 - N_2)\mu B = (N - 2N_1)\mu B, \tag{1.2}$$

where N_1 is the number of spin particles aligned parallel to the field, N_2 is the number of spin particles aligned anti parallel to the field and $N_1 + N_2 = N$. We use Eq.(1.2) in the discussion of entropy and temperature of the system.

1.2 Entropy

Entropy is a quantity that measures the degree of randomness or disorder of a system. It forms the fundamental bridge between the macroscopic thermodynamic quantities and the microscopic variables which in the realm of statistical mechanics is a function of the probabilities whereas within classical thermodynamics, it is the state function demanded by the Second Law [1]. The basic formula which ties the two variables was achieved by Ludwig Boltzmann (carved on his tombstone in Vienna) as:

$$S = k_B \ln \Omega_i, \tag{1.3}$$

where S is entropy of the macroscopic quantity describing the system, Ω_i is the number of accessible microstates of the system and k_B is Boltzmann's constant. In relation to the number of accessible states, entropy is the quantitative measure of disorder in the relevant distribution of the system over its permissible microstates [2]. Mathematically, the number of accessible states, Ω_i, for the N spin-half particles system we are considering above is given by

$$\Omega_i = \frac{N!}{N_1!N_2!}. \tag{1.4}$$

To simplify this expression further, let's measure the energy of the system by setting its ground state energy to zero. So, each N_1 spin-half particles in the ground state has zero energy and each N_2 particles in the excited state has energy equal to $2\mu B$. This implies that

$$N_2 = \frac{E}{\Delta} \qquad and \qquad N_1 = N - \frac{E}{\Delta}. \tag{1.5}$$

With these new variables Eq.1.4 can be rewritten as

$$\Omega_i(E, \Delta) = \frac{N!}{(N - \frac{E}{\Delta})!(\frac{E}{\Delta})!}. \tag{1.6}$$

Next, we define the entropy per particle $s(u, \Delta)$ for the system as [4]

$$s(u, \Delta) = \lim_{E,N\to\infty;\frac{E}{N}=u} \frac{k_B}{N} \ln \Omega_i(E, \Delta). \tag{1.7}$$

Applying Stirling's approximation to Eq.1.7, $s(u, \Delta)$ becomes

$$s(u, \Delta) = -\frac{u}{\Delta} \ln(\frac{u}{\Delta}) - (1 - \frac{u}{\Delta}) \ln(1 - \frac{u}{\Delta}), \tag{1.8}$$

where k_B is set to 1.

Eq.1.4 or 1.6 implies that when all the particles are in a single state, either in the ground state ($N_1 = N$) or in the excited state ($N_2 = N$), entropy is zero. In between these two, starting from the ground state, entropy of the system begins to increase from zero value, attains a certain maximum value and then begins to decline until it reaches zero again.

From the point of view of Eq.1.8, when all the spin-half particles are in the ground state, u is zero; all the particles are in the ground state in which only a single state is accessible. As a result Ω_i is unity. Both from calculation of the number of states accessible to the system or from the computation of Eq.1.8, the entropy per particle is zero. An increase from the ground state energy of the system means that a corresponding amount of particles will occupy the excited state. This increases the internal energy per particle u and as a result entropy per particle increases. As u increases from zero to 0.5Δ, entropy on its turn increases from zero to $s_{max} = \ln 2$- the maximum entropy per particle. This maximum entropy per particle corresponds to state where there are equal number of particles in the ground and in the excited states.

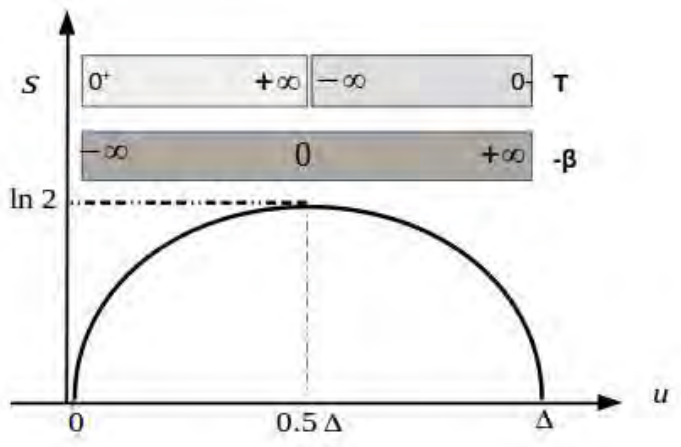

Figure 1.2: Entropy per particle versus energy per particle for ideal spin-half particles.

Once there are equal number of spin-half particles in the ground and excited states, further increase in energy makes the excited state to be more populated than the ground state. This, in turn, results in a decrease in Ω. In other words, as energy per particles

increases from 0.5Δ to Δ, entropy per particle, s, decreases from its maximum value s_{max} to zero. When $u = \Delta$, all the spin-half particles are already in a single excited state-only one accessible state. Hence, entropy per particle is again zero. Beyond the state $u = 0.5\Delta$, where more number of particles in the excited state than in the ground state, population inversion, a phenomenon in which more particles occupy the excited state than the ground state, takes place. In this region, the change in entropy per particle with energy per particle becomes negative. Thermodynamics defines absolute temperature as $T^{-1} = \partial S/\partial E$ [3, 4].

Fig.1.2 shows the entropy per particle versus energy per particle for a system of spin-half particle. Entropy per particle increases from 0 to $\ln 2$ in the left-half, and decreases from $\ln 2$ to 0 in the right-half part. The plots of Temperature in the kelvin scale and inverse temperature parameter(its negative), $-\beta$, versus energy per particle are also shown on the top part of the curve. In the next subsections we will discuss temperature in more details.

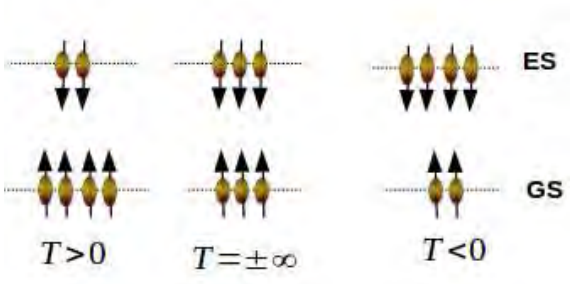

Figure 1.3: Population inversion in a spin-half system of six spin particles [5]. In the case where $T > 0$ (left), more number of spins (four) are in the lower (ground, GS) state than (two) in the higher (excited state, ES). Whereas in the case $T = \pm\infty$ (middle plot), both lower and upper states are equally populated. On the other hand, when absolute temperature is negative, excited state is more populated than in the ground state.

Fig.1.3 shows how temperature varies with the state of spin-half system. The left plot where more number of particles are in the lower (ground) state than in the upper (excited) state, the temperature of the system is positive finite. In the middle in which the population of particles in both states is equal, the temperature of the system is infinity. The right plot shows the case where more particles occupy the higher state than the lower; the temperature of the system becomes negative.

The discussions of thermodynamic quantities in this work are solely of a two-level sys-

tem. However, one can extend it to systems (multi-level) capable of exhibiting negative absolute temperature. In the subsequent subsections, we present these quantities in relation to a system of two-level (spin-half) particles.

1.3 Negative absolute temperature

Absolute temperature is the fundamental temperature scale and in most natural systems it is usually bound to be positive [6]. It is one of the central concepts of statistical mechanics and thermodynamics. Kelvin defined the absolute temperature scale in such a way that nothing could be colder than absolute zero. Physicists later realized that the absolute temperature of a gas is related to the average energy of its particles. Accordingly, absolute zero temperature is taken as the state in which all particles of a given system have no energy at all and as a result all motions in system ceases whereas higher temperatures correspond to higher average energies. Physicists started being challenged with a class of systems and they realized this assumption is **not** always possible, especially with the case in which higher energy assumed to correspond to positive temperature alone. However, in some systems higher energy does not necessarily corresponds to positive temperatures- the cause believed to be the beginning of the study of negative absolute temperature.

The concept of negative absolute temperature was originally introduced by a Norwegian chemist and physicist Lars Onsager [7]. However, they were E.M Purcell and R. V. Pond [8] who conducted an experiment on a nuclear spin system at negative absolute temperature and studied various properties of spin nuclear system in pure LiF (a compound with long relaxation time in both strong and weak magnetic fields). But, Ramsey is known to have developed the principle of negative absolute temperature in thermodynamics and statistical mechanics [9].

Very recently, the study of absolute negative temperature has gained interest by theoretical and experimental physicists. A couple of experimental works and theoretical illustrations demonstrate that negative absolute temperature is achievable, see [6, 8, 9, 10] and references therein. However, study shows achieving negative absolute

temperature is not by removing the energy from a system; rather it is by adding more and more energy to a class of matter which has the quality whose thermodynamic entropy is not a monotonically increasing function of its internal energy [8, 9]. In the possible range of entropy (in which $\partial S/\partial E < 0$), the addition of energy to a system capable of negative absolute temperature would make them more orderly, decreasing entropy and results in negative absolute temperature, see Fig.1.2. The expression for temperature from Eq.1.8 is

$$\frac{1}{T} = \frac{1}{\Delta} \ln(\frac{\Delta}{u} - 1). \tag{1.9}$$

It is straight forward to see that in the range from 0 to s_{max}, temperature the inverse of the slope of s versus u curve is positive. At the value when $\Delta = 0^+$, T^{-1} is $+\infty$ and $T = 0$. T increases from 0^+ to $+\infty$ in this range. As the energy level spacing, Δ increases from 0.5Δ to Δ, temperature is negative and increases from $-\infty$ to 0^-. But most naturally occurring systems including a classical gas are limited to positive absolute temperatures. Only a special class of matter which have an upper bound for the energy E_{max} of its particles is able to reach negative absolute temperatures. This maximum possible energy corresponds to a limit after which the system stops absorbing more energy even if there is plenty of available energy [11]. In the following subsections, we discuss how entropy and temperature of such a spin system changes when energy is added to it.

1.3.1 Negative absolute temperature and entropy of the system

If infinitesimally small energy is added to the system per particle when it has equal population in the ground and excited states, some more particles will occupy the excited state by leaving the ground state. Since the occupation of the higher state in this case leads the system to a more orderly state, its entropy per particle begins to decrease, though energy is being added to it. With the addition of more energy per particle, the entropy per particle of the system decreases further. Finally, when the system attains maximum possible energy, all the particles occupy only the excited state, leaving the ground state vacant. In this case a single excited state is occupied; similar to the case

of the ground state, Ω_i, the number of accessible state is unity and entropy is zero again. This is similar to the case where all the particles are occupying the ground state with one basic difference: in the former case it is the beginning for entropy to increase; in the later case it is the end of decreasing entropy.

When a small amount of energy per particle is added to the system which is already at positive infinite temperature, its temperature abruptly changes to negative infinity. In other words, the slope of the entropy-energy curve changes from a very small positive (+0) value to the same value with opposite sign. A spin-half system at temperatures $T = \pm\infty$ describe physically the same distribution and same values of thermodynamic quantities except for temperature [11]. As energy per particle of the system increases from 0.5Δ to Δ, the temperature of the system also increases (from -∞ to -0). When the energy per particle of the system attains its maximum value ($u = \Delta$), **all** particles occupy the excited state. The entropy versus energy curve becomes vertical; temperature of the system becomes zero; however, it comes from negative value. So for systems which are capable of describing negative absolute temperature, entropy versus energy curve forms some sorts of symmetry.

Figure 1.4: Absolute temperature (T) and inverse temperature (1/T) versus energy for a spin-half system.

Fig.1.4 shows absolute temperature and inverse thermodynamic beta of particles in a given state versus energy per particle for spin-half system. T is the absolute temperature and 1/T is thermodynamic beta of the system.

1.3.2 Thermodynamic Beta ($\beta \propto T^{-1}$)

β sometimes called thermodynamic beta is the reciprocal of the absolute temperature of a system (k_B is set to one) with a unit of inverse of joule. It describes the change in entropy to change in energy ($\beta = k_B^{-1}\partial S/\partial E$). Unlike T, beta is a continuous variable over the entire range of energy. This makes beta to be considered as a more fundamental and a preferable quantity in statistical and thermal physics than temperature. As energy per particle increases from 0 to 0.5Δ, β decreases from $+\infty$ to zero; as u increases from 0.5Δ to Δ, then β decreases further from zero to $-\infty$. Taking the advantage of $\beta's$ continuity in the entire range of energy, in this work we use beta instead of temperature in the expressions of thermodynamic quantities. We suggest that it makes sense if β had been defined as the negative of the inverse of temperature T ($\beta \propto -T^{-1}$). If that had been the case, beta would have been running from $-\infty$ to $+\infty$ smoothly and could have matched with our notion of the number line (see an increasing solid line in the entire u range of Fig.1.4).

1.4 Heat engine with negative absolute temperature

Heat engine is a device that is capable of cyclically converting thermal energy to useful work. However, due to dissipations, real heat engines do not convert all of the thermal energy they absorb to useful work. Under a very ideal situation of quasistatic operations, which can be taken as reversible process, heat engines can not convert all the thermal energy they absorb to useful work. In such a working condition, they would be very efficient. The problem with such operation is that the power at which they do the energy transduction is practically zero and hence quasistatic mode of operation does not represent a real heat engine. A good example of quasistatic efficiency is

the famous Carnot efficiency, $\eta_c = 1 - \frac{T_c}{T_h}$ where $T_h > T_c > 0$. Heat engines can also operate at a maximum power; but they can not be as efficient as that of the quasistatic.

In the times when energy resource is so meager, heat engines with minimum efficiency are not in need. Heat engines need to operate at finite-time and the speed of the thermodynamic cycles should be finite to produce non-zero finite power. Therefore, it is important to investigate how large the efficiency of a heat engine can be reached when the engine operates in the region of maximum power. One important finding that is considered as universal is the Curzon–Ahlborn efficiency, $\eta_{CA} = 1 - \sqrt{\frac{T_c}{T_h}}$, which is the efficiency at maximum power for a macroscopically endoreversible heat engine operating between a cold bath at temperature T_c and a hot bath at temperature T_h (with $T_h > T_c > 0$) [13, 14].

Based on the working substance used, heat engines can be classified as classical or quantum mechanical heat engines. Classical heat engines use for example gas filled cylinders as a working substance whereas quantum heat engines employ multi-level quantum systems. Common heat engines both classical or quantum mechanical run cyclically between two thermal reservoirs at two positive distinct temperatures T_1 and T_2.

Recent advances in experimental and observational techniques have made it possible to study many-particle systems that can be thermally decoupled from their environment [15]. Spin systems with bounded energy [8] and ultra-cold quantum gases [6] are good examples. These systems are stable and capable of demonstrating negative absolute temperature. In addition, such experiments concerning the consequences of matter at negative absolute temperature is recently studied by S. Braun *et.al* [11]. As studies show, a working substance for a heat engine would have the possibility to absorb heat energy from a reservoir at absolute positive and negative temperatures. However, it is difficult to adiabatically cross from positive to negative (or from negative to positive) absolute temperature. As a result, it is either very difficult or impossible to construct a heat engine that operate between a positive and a negative absolute temperature. Unlike the way it was defined in reference [16] in which efficiency is reported being

greater than one -a violation of energy conservation, efficiency of a heat engine can not be greater than unity.

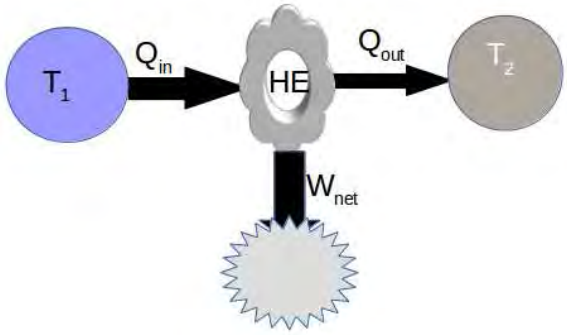

Figure 1.5: Schematic diagram of a model heat engine.

In the study of a system capably of demonstrating negative absolute temperature, some terms and concepts are not clear and may lead to misconceptions. It should be clear that negative absolute temperature systems are not colder than absolute zero; no natural or scientifically prepared system can have temperature colder than absolute zero Kelvin. To avoid the discontinuity of absolute temperature at maximum entropy, we have chosen to use the continuous variable β for the remaining part of our work.

Previously, a number of heat engines which operate between two distinct positive temperatures have been studied with broad category of quantum and classical heat engines. Most of the quantum mechanical heat engine studies have focused on the quantum analogue of classical Carnot engine and description of quantum thermodynamical processes [17, 18, 19, 20]. Studies on the classical heat engines have focused on Carnot efficiency and maximum power, for example, see references [13, 14, 21, 22]. None of these heat engines could be modeled neither as a heat engine that may be optimized and operate between two positive temperature reservoir nor as a heat engine that operates between negative temperature reservoirs. However, the fact that a system of spin-half particles are stable at negative absolute temperature and the possibility that a heat engine can operate between either both positive or both negative temperatures open a new option for a heat engine. As this area of study is demanding, we have described its quasistatic and finite-time processes. In particular, thermodynamic quantities such as power and efficiency of the heat engine in the finite-time scenario needs investigation. Besides the

efficiency benefit, the heat engine we are exploring can be optimized by employing a unified optimization criterion for any energy converters which have been proposed by A. C. *Hernánadez et.al* [23]. Using parameters of the model, we search for points where the engine operates as a heat engine. The *figure of merit* proposed for the engine shows optimized mode operation to be better than its operations at maximum power mode.

Room temperature of 300 K and k_BT are, respectively, chosen to scale temperature and energy; all values and numerical figures presented in this work are given in terms of these units.

The rest of the thesis is organized as follows. In Chapter 2, model engines and quasistatic thermodynamic processes are described. We derive the quasistatic thermodynamic quantities such as net heat absorbed and quasistatic efficiency. In Chapter 3, descriptions of finite-time mode of operation and the corresponding thermodynamic processes are presented. Net finite heat absorbed, power and efficiency and thermodynamic quantities at the maximum power mode of operation are derived. In Chapter 4, optimized modes of operations are explored: optimized power, optimized efficiency and figure of merit for the models are determined. Finally, summary and conclusion are given in Chapter 5.

Chapter 2

Model of the system and quasistatic thermodynamic processes

In this Chapter we describe our model heat engines while working under the quasistatic condition whose working substances are systems of spin-half particles. In particular, we use the systems of spin-half particles under the simplified assumptions that they are very weakly interacting with each other and fixed in position. The quasistatic processes refer to an extremely slowly changing process where the system is continuously changing from one equilibrium state to the next. From the quasistatic thermodynamic processes, the corresponding thermodynamic quantities such as net work done, power and efficiency are derived.

2.1 Model description

We consider a system of two-level spin-half particles of excited (ground) state $|e>$ ($|g>$) which are fixed in position and have instantaneous eigen-energy $E_e(E_g)$ in a varying external magnetic field. Moreover, it interacts with heat baths of positive inverse temperatures $\beta_{1(5)}$ and $\beta_{2(6)}$ in which $\beta_{2(6)} > \beta_{1(5)}$ in regions I(III) and in region II, the system of spin-half particles interacts with heat baths of negative inverse temperatures β_3 and β_4 where $\beta_3 > \beta_4$ ($|\beta_3| < |\beta_4|$), see Fig.2.1.

Initially, the system (while it is in an external magnetic field) is kept in thermal equilibrium with a heat reservoir at temperatures β_s where s is either 1, 3 or 5 which signifies the temperatures of the hotter (1 for I and 5 for III) reservoirs and of the

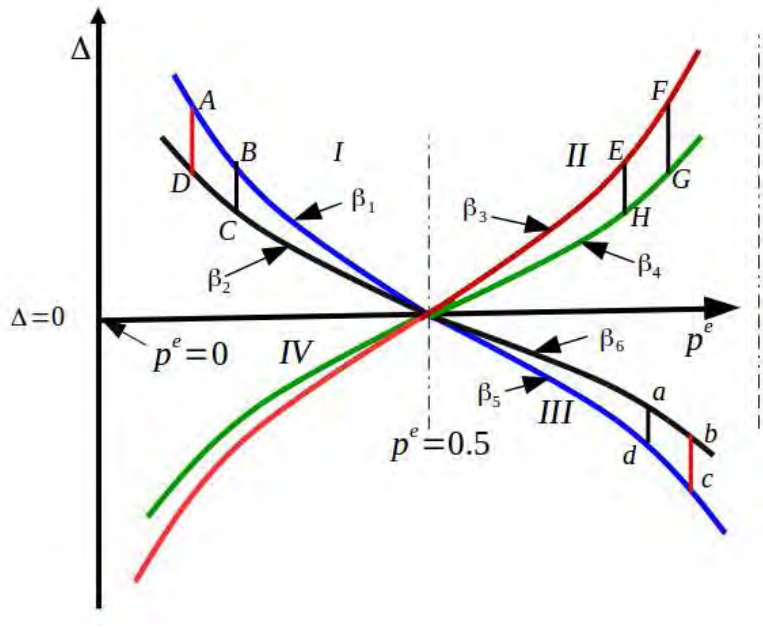

Region	p^e range	Δ	β
I	0-0.5	+ve	+ve
II	0.5-1	+ve	-ve
III	0.5-1	-ve	+ve
IV	0-0.5	-ve	-ve

Figure 2.1: Schematic diagram of the three model engines working between reservoirs under quasistatic mode of operations. The energy level spacing versus occupation probability in the excited state is plotted from $\Delta = (1/\beta_r)ln((1-p^e)/p^e)$, where r assumes numbers from 1-6 depending on the inverse temperature of the reservoir. In regions I and III, the $\beta's$ are all positive and in region II, however $\beta's$ are negative.

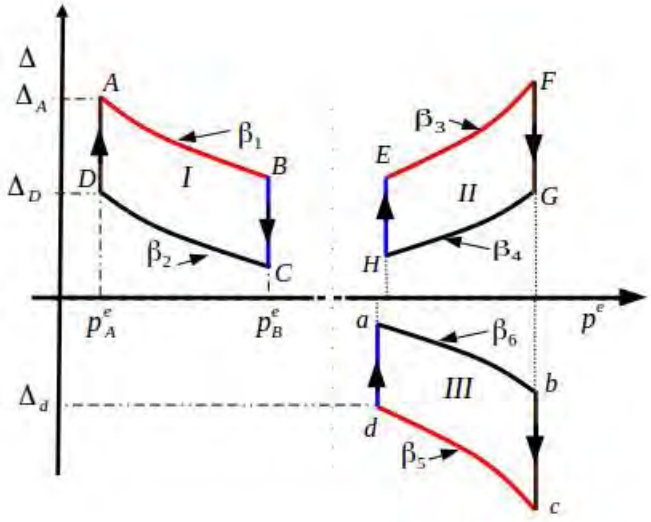

Figure 2.2: Schematic diagram of the three model engines working between reservoirs under quasistatic mode of operations: models I and III represent model engines which operate between two reservoirs at positive temperatures (the energy level spacing $\Delta's$ are positive for model I and negative for model III). In model II the the temperatures of the reservoirs are both negative and the energy level spacings are positive. The curves represent isothermal processes and vertical segments show adiabatic changes.

colder reservoir for model II. The heat exchange and the corresponding work done on (by) the system changes the occupation probability and the energy level spacing. The level spacing which is the energy difference between the excited and the ground states of the system changes in proportion to the change in external field. The absorption (release) of heat should be in an extremely very slow fashion to ensure that the system always remains in equilibrium states during the isothermal processes.

In the quasistatic isothermal changes, the system is in thermal equilibrium with the reservoirs, and obeys the Gibbs distribution function which can be simplified to give

$$p_i^e = \frac{1}{1 + e^{\beta_r \Delta_i}}, \tag{2.1}$$

where p_i^e is the occupation probability in the excited state of equilibrium state i, β_r is inverse temperature of the bath which the system is in contact with, $\beta_r \propto 1/T$ and $\Delta_i = E_i^e - E_i^g$. The superscript e and g denote excited and ground states, respectively. One can find the level spacing, Δ, to change with occupation probability in the excited state p_i^e to be given by

$$\Delta_i = \frac{1}{\beta_r} \ln(\frac{1 - p_i^e}{p_i^e}). \tag{2.2}$$

For our model Δ_i can assume positive, zero or negative value depending on the orientation of the external magnetic field.

2.2 Internal energy, work and heat exchange in the spin-half system

As a prerequisite for the subsequent discussion, we first derive fundamental relations which we employ to find thermodynamics quantities such as internal energy, work done and heat exchange. For this, we consider the mean internal energy per particle,$\langle u \rangle$, of the spin half system which is described as

$$\langle u \rangle = \sum_i E_i p_i \tag{2.3}$$

where p_i is the occupation probability of the i^{th} state, E_i is its corresponding energy eigen-value per particle. The summation i runs over the excited and ground states.

By taking an infinitesimal change in the mean internal energy per particle, we can get expression for work done and heat absorbed from

$$d\langle u\rangle = \sum_i [E_i dp_i + p_i dE_i] \tag{2.4}$$

where the first term of this Eq.2.4 is an infinitesimal energy change in the form of heat $dQ = \sum_i E_i dp_i$ while the second term is infinitesimal energy change in the form of work $dW = \sum_i p_i E_i$ so that

$$d\langle u\rangle = dQ + dW. \tag{2.5}$$

However, for a general process, dQ can be decomposed into two parts:

$$dQ = đQ + dQ_{irr} \tag{2.6}$$

where $đQ$ is the part where a system interacts thermally with an external world while dQ_{irr} is a dissipative thermal energy a system acquires due to an irreversible process. In a similar way, dW, can be decomposed into two parts:

$$dW = đW + dW_{irr} \tag{2.7}$$

where the first term $đW$ is a system's interaction energy with external world via work while the second term, dW_{irr}, is the energy a system gets work-wise due to an irreversible process.

On the other hand, from the first law of thermodynamics:

$$d\langle u\rangle = Q + W. \tag{2.8}$$

Comparing Eq.2.5 with 2.8, we then have

$$dQ_{irr} + dW_{irr} = 0 \tag{2.9}$$

However, from second law of thermodynamics dQ_{irr} is **positive** since there is heat generation during any irreversible process. Hence, $dW_{irr} < 0$ in order to satisfy Eq.2.9.

We will make use of Eqs.2.6 and 2.7 later in Chapter 3 when we deal with Finite-time processes which involve irreversible work and heat.

In the quasistatic processes of this chapter, there are no irreversible heat and work. For the system of spin-half particles we are considering, the heat exchange is then

$$dQ = E_e dp_e + E_g dp_g = \Delta dp_e \tag{2.10}$$

where $\Delta = E_e - E_g$, $p_e + p_g = 1$. The work done can then be written as

$$dW = p_e d\Delta \tag{2.11}$$

The quasistatic heat exchanged Q^q and the work done W^q in the continuum limit are obtained by integrating Eqs. 2.10 and 2.11, respectively, as

$$Q^q = \int_{p_0^e}^{p_f^e} \Delta_E dp_e, \tag{2.12}$$

$$W^q = \int_{\Delta_0}^{\Delta_f} p_e d\Delta_i, \tag{2.13}$$

where Δ_i and β are as defined in Sec.2.1 while $\{p_0^e, \Delta_0\}$ and $\{p_f^e, \Delta_f\}$ are, respectively, the initial and final states of the system. The last two equations will be used in the remaining parts of our work.

2.3 Thermodynamic quantities and processes (models I and III)

A thermodynamic process is a change of thermodynamic system from one (initial) to another (final) state. There are two fundamental processes that take place in each of the processes per cycle: isothermal and adiabatic processes. An isothermal process is a change due to exchange of heat between the system and the reservoirs which takes place at constant temperature. During the isothermal processes, the occupation probability in the excited state changes. On the other hand, adiabatic processes are processes which take place without any exchange of heat between the system and the reservoirs; by increasing or decreasing the external magnetic field, the system either does work on the reservoirs or the reservoir does work on the system.

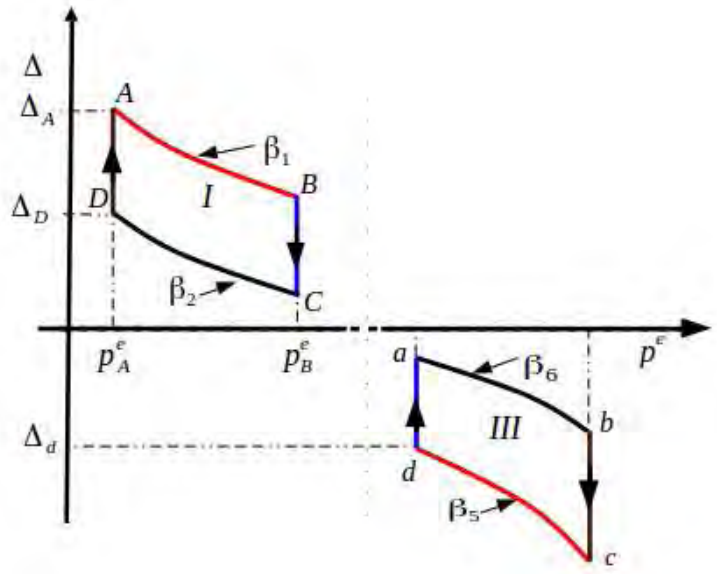

Figure 2.3: Schematic diagram of the model engines working between two positive temperatures for quasistatic processes: model I represents when the energy level spacing $\Delta's$ are positive; whereas model III shows when $\Delta's$ are negative. In both sketches, the curves represent isothermal processes and vertical segments show adiabatic changes.

2.3.1 Quasistatic isothermal processes (models I and III)

In quasistatic isothermal processes, the system of spin-half particles is kept in thermal contact with a reservoir at constant temperature. By absorbing heat from the reservoir, work is done by the system. Or equivalently, the environment may also do work on the system while the system is releasing heat. This results in a simultaneous change of both the occupation probability and the energy level spacing of the system; however, the system remains in thermal equilibrium.

Fig. 2.3 describes cyclic thermodynamic processes. The curves representing two different quasistatic isothermal processes (for each model) are plotted using Eq. 2.2. In the models, curves AB and ab represent isothermal processes in which the occupation probability of the excited state increase, respectively, from p^A to p^B and p^a to p^b. Similarly, curves CD and cd represent other isothermal processes in which the occupation probability of the excited state decreases, respectively, from p^C to p^D and p^c to p^d. Vertical segments represent adiabatic changes. For the purpose of brevity, in the subsequent sections, we drop the the subscript e from the occupation probability, p_e, that

has been used to indicate 'excited' as it does not bring any confusion after all.

The quasistatic isothermal process A→B and a→b

In the context of our model, in the quasistatic isothermal processes A→B (model I) and a→b(model III) the occupation probability of the system increase due to the exchange of heat between the system and the reservoirs.

We begin the description of isothermal processes (model I) in the case where the system is initially at A $\{p^A, \Delta_A\}$ in an external magnetic field whose magnitude is relatively large as compared to its value at point C $\{p^C, \Delta_C\}$, see Fig.2.3. Assisted by a varying external magnetic field, the spin-half system changes isothermally from the initial state $\{p^A, \Delta_A\}$ to the final state $\{p^B, \Delta_B\}$ where p^A, p^B are, respectively, the occupation probabilities of the initial and final excited states while Δ_A and Δ_B are, respectively, the energy level spacing of the initial and final states. The external magnetic field should extremely slowly change to ensure quasistatic process. As the system absorbs heat from the reservoir and does work, its occupation probability of the excited state increases. As the external magnetic field decreases, the level spacing of the system also decreases. In the course of decreasing the energy level spacing from Δ_A to Δ_B , the occupation probability of the excited state increases from p^A to p^B according to

$$\Delta_i = \frac{1}{\beta_1} \ln(\frac{1-p_i^e}{p_i^e}). \tag{2.14}$$

The quasistatic heat absorbed, $Q^q_{in}(I)$, in the quasistatic isothermal process $A \rightarrow$B, is then simply the area under $A \rightarrow$B curve ($Q^q_{AB}(I) = \int_{p^A}^{p^B} \Delta_i dp_i$). After integration, the heat absorbed in this isothermal process turns oot to be:

$$Q^q_{AB}(I) = \frac{1}{\beta_1}[p^B \ln(\frac{1-p^B}{p^B}) - p^A \ln(\frac{1-p^A}{p^A}) + \ln(\frac{1-p^A}{1-p^B})]. \tag{2.15}$$

The quasistatic work done, $W^q_{AB}(I)$, by the system in process $A \rightarrow$B becomes

$$W^q_{AB}(I) = \Delta_B - \Delta_A + \frac{1}{\beta_1} \ln(\frac{1+e^{\beta_1 \Delta_A}}{1+e^{\beta_1 \Delta_B}}). \tag{2.16}$$

For model III, a similar procedure can be followed except that the orientation of the magnetic field is opposite to that of the field used in model I. One can begin from

state $\{p^a, \Delta_a\}$ and then isothermally (and quasistatically) changes the system to state $\{p^b, \Delta_b\}$.

The quasistatic heat released, $Q^q_{ab}(III)$, in the quasistatic isothermal process $a \rightarrow$b, is then simply the area above curve $a \rightarrow$b and the p^e axis.

$$Q^q_{ab}(III) = \frac{1}{\beta_6}[p^b \ln(\frac{1-p^b}{p^b}) - p^a \ln(\frac{1-p^a}{p^a}) + \ln(\frac{1-p^a}{1-p^b})]. \tag{2.17}$$

The quasistatic work done, $W^q_{ab}(III)$, by the system in process $a \rightarrow$b becomes

$$W^q_{ab}(III) = \Delta_b - \Delta_a + \frac{1}{\beta_6} \ln(\frac{1+e^{\beta_6 \Delta_a}}{1+e^{\beta_6 \Delta_b}}) \tag{2.18}$$

2.3.2 The adiabatic processes B→C and b→c

In model I, such an adiabatic process is a sudden change in which the system of spin-half particles, previously in contact with the β_1 reservoir, is now disconnected and suddenly reconnected to the β_2 reservoir, see Fig.2.3. Here, we decrease further the magnitude of the external magnetic field without altering its direction. Due to the sudden change in the external magnetic field, the energy level spacing instantly shifts from Δ_B to Δ_C. There is no heat exchange between the system and the reservoir. The work done, W_{BC}, by the system in $B \rightarrow$C is

$$W_{BC} = p^B(\Delta_C - \Delta_B). \tag{2.19}$$

In model III, the system of spin-half particles is suddenly disconnected form the β_6 reservoir and then is connected to the β_5 reservoir, see Fig.2.3(model III). The magnitude of the external magnetic field increases further without altering its direction. Due to the sudden change in the external magnetic field, the energy level spacing instantly shifts from Δ_b to Δ_c. Note that in this region the energy level spacing is negative. The work done, W^q_{bc}, by the system in $b \rightarrow$c is

$$W_{bc} = p^b(\Delta_c - \Delta_b). \tag{2.20}$$

In both cases however, the occupation probability of the system does not change during the adiabatic processes. It should be noted that the operational time of an adiabatic process is very short; negligibly small compared to that of the time for quasistatic

isothermal processes. So, the adiabatic changes, both in I and III, are not quasistatic processes rather they are finite-time processes.

2.3.3 The quasistatic isothermal processes C→D and c→d

In such isothermal processes, the occupation probability of the system in the excited state decreases while the system is exchanging energy in the forms of heat and work with the reservoirs. This process should be very slow so that the system remains arbitrarily close to equilibrium at all times (during its interaction with the reservoirs).

Quasistatic isothermal processes C→ D and c→d

These processes start after the previous adiabatic processes B→C . In model I, once the system is brought in thermal contact with the β_2 reservoir and relaxes to equilibrium, then it is ready for the next isothermal process wherein it changes its state from $\{p^C, \Delta_C\}$ to a state with lesser occupation probability of the excited state, $\{p^D, \Delta_D\}$. Here, the external magnetic field increases (opposite to process AB) extremely slow enough to meet the demand of quasistatic process. During this quasistatic change the occupation probability in the excited state decreases as the system releases heat to the reservoir. So, the heat released $Q^q_{CD}(I)$, in process $C \rightarrow$D, is

$$Q^q_{CD}(I) = \frac{1}{\beta_2}[p^A \ln(\frac{1-p^A}{p^A}) - p^B \ln(\frac{1-p^B}{p^B}) + \ln(\frac{1-p^B}{1-p^A})]. \tag{2.21}$$

Due to the change in the energy level spacing in the process $C \rightarrow$D, quasistatic work $W^f_{CD}(I)$, is done on the system:

$$W^q_{CD}(I) = \Delta_D - \Delta_C + \frac{1}{\beta_2} \ln(\frac{1+e^{\beta_2 \Delta_C}}{1+e^{\beta_2 \Delta_D}}) \tag{2.22}$$

In model III, the system is brought in thermal contact with the β_5 reservoir(see Fig.2.1) and relaxes to equilibrium and then undergoes the change from a state $\{p^c, \Delta_c\}$ to state with lesser occupation probability of the excited state, $\{p^d, \Delta_d\}$. To conduct the process, it suffices to decrease the magnitude of the magnetic field. During this quasistatic change the occupation probability in the excited state decreases. This process enables the magnitude of the energy level spacing and the occupation probability of the excited

state to decline, bringing the system to another state $\{p^d, \Delta_d\}$, see Fig. 2.1. So, there is energy exchange between the system and the reservoir. In the quasistatic isothermal process C→D, the heat released, $Q^q_{CD(I)}$, by the system is

$$Q^q_{cd}(III) = \frac{1}{\beta_5}[p^c \ln(\frac{1-p^c}{p^c}) - p^d \ln(\frac{1-p^d}{p^d}) + \ln(\frac{1-p^c}{1-p^d})]. \tag{2.23}$$

The corresponding work done, W^q_{cd}, on the system can be shown to be

$$W^q_{cd}(I) = \Delta_d - \Delta_c + \frac{1}{\beta_5} \ln(\frac{1+e^{\beta_5 \Delta_c}}{1+e^{\beta_5 \Delta_d}}) \tag{2.24}$$

2.3.4 Adiabatic process D→A and d→a

In model I, when the system reaches a state at D, it is suddenly disconnected from the reservoir at inverse temperature β_2 and then immediately reconnected back to the reservoir at inverse temperature β_1 . This process increases the energy level from Δ_D to Δ_A and thereby returning the system back to the initial state. The work done, $W_{DA}(I)$, on the system during this adiabatic change is then simply

$$W_{DA}(I) = p^A(\Delta_A - \Delta_D). \tag{2.25}$$

In model III, when the system reaches a state at d, it is also suddenly disconnected from the reservoir at inverse temperature β_5 and then immediately reconnected back to the reservoir at inverse temperature β_6 . This process increases the energy level from Δ_d to Δ_a. This adiabatic process takes the system back to the original state and one cycle is said to be completed. The work done, $W_{da}(III)$, on the system during this adiabatic change becomes

$$W_{da}(III) = p^a(\Delta_a - \Delta_d). \tag{2.26}$$

2.3.5 Net heat absorbed and quasistatic efficiency

In model I, the system absorbs heat in process AB and releases in process CD. Therefore, the net heat absorbed $Q^q_{net}(I)$ per cycle can be calculated as $Q^q_{net}(I) = Q^q_{AB}(I) + Q^q_{CD}(I)$. Hence,

$$Q^q_{net}(I) = \alpha(p^B \ln(\frac{1-p^B}{p^B}) - p^A \ln(\frac{1-p^A}{p^A}) + \ln(\frac{1-p^A}{1-p^B})), \tag{2.27}$$

where $\alpha = \beta_1^{-1} - \beta_2^{-1}$. Note that the net heat exchanged is positive and hence the model acts as an engine. It is simple to verify that the net work done $W^q_{net}(I) = -Q^q_{net}(I)$. The quasistatic efficiency of the system, $\eta^q(I)$ under the quasistatic mode of operation can be obtained by taking the ratio of the net heat absorbed to the heat absorbed by the by the system. Hence, $\eta^q(I) = Q^q_{net}(I)/Q^q_{in}(I)$. Using Eqs. 2.15 and 2.27, $\eta^q(I)$ becomes

$$\eta^q(I) = 1 - \frac{\beta_1}{\beta_2}. \tag{2.28}$$

The net heat absorbed by the systenm in model III can be computed by adding Eqs. 2.17 and 2.23 to get

$$Q^q_{net}(III) = Q^q_{cd}(III) - \frac{\beta_5}{\beta_6} Q^q_{cd}(III). \tag{2.29}$$

The quasistatic efficiency of the system, $\eta^q(III)$, which is the ratio of the net heat absorbed, $\mathrm{Q}^q_{net}(III)$, to the heat absorbed, $\mathrm{Q}^q_{cd}(III)$ the system can be written in a simple form using Eqs. 2.15 and 2.27, $\eta^q(I)$. So,

$$\eta^q(III) = 1 - \frac{\beta_5}{\beta_6}. \tag{2.30}$$

2.4 Thermodynamic quantities and processes (model II)

Description of thermodynamic processes and quantities given in Sec.2.3 apply also to the description of models engines which operate between heat reservoirs with negative inverse temperatures. Hence, we do not give detailed explanation for this section; rather we elaborate isothermal and adiabatic processes.

2.4.1 Quasistatic isothermal process (model II)

In quasistatic isothermal processes, the system of spin-half particles is kept in thermal contact with a reservoir at constant temperature. By absorbing heat from the reservoir,

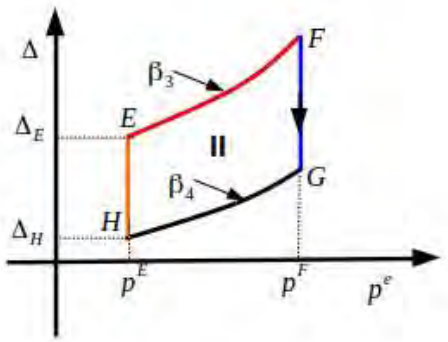

Figure 2.4: Schematic diagram of the model engine working between two absolute negative temperatures for quasistatic processes. The inverse temperature parameter $\beta's$ are negative. Smooth curves represent isothermal processes and vertical segments, connecting the curves, represent adiabatic processes.

work is done by the system. Or equivalently, the environment may also do work on the system while the system is releasing heat. This results in a simultaneous change of both the occupation probability and the energy level spacing of the system; however, the system should remain in thermal equilibrium. Note that the two fundamental processes discussed under models I and III apply for the model engine we are going to discuss. The only difference is that the the reservoirs for these models are at negative absolute temperatures.

Fig. 2.4 describes cyclic quasistatic thermodynamic processes in which a heat engine operates between two negative temperatures. The curves representing two different quasistatic isothermal processes are plotted using Eq.(2.2). In the model, curves EF and GH represent isothermal processes. The vertical axis represents the energy level spacing Δ_i and the horizontal one represents the occupation probability in the excited state p_i^e. The vertical segments, connecting the curves, represent adiabatic changes. $\beta's$ are inverse negative absolute temperatures of their respective heat reservoirs with $\beta_3 > \beta_4$.

The quasistatic isothermal process E→F

We describe isothermal and adiabatic processes for such a model engine in a similar manner to a heat engine working between two positive temperatures. Suppose that the system is initially at state E, $\{p^E, \Delta_E\}$, in an external magnetic field whose magnitude

is relatively small as compared to its value around point F ($\{p^F, \Delta_F\}$, see Fig.(2.4). By increasing the magnitude of the external magnetic field to which the system is subjected, the spin-half system changes isothermally (and quasistatically) from this initial state to the final state $\{p^F, \Delta_F\}$ where p^E, p^F are,respectively, the occupation probabilities of the initial and final excited states while Δ_E and Δ_F , respectively, are the energy level spacing of the initial and final states. As the system absorbs heat from the reservoirs, the occupation probability in the excited state increases.
The quasistatic heat absorbed Q^q_{EF} between the system and the reservoir in the isothermal process E$\rightarrow F$ is

$$Q^q_{in} = \frac{1}{\beta_3}[p^F \ln(\frac{1-p^F}{p^F}) - p^E \ln(\frac{1-p^E}{p^E}) + \ln(\frac{1-p^E}{1-p^F})]. \tag{2.31}$$

The work done, W^q_{EF}, by the system in this isothermal process work is

$$W^q_{EF} = \Delta_F - \Delta_E + \frac{1}{\beta_3} \ln(p^F/p^E). \tag{2.32}$$

where β_3 is the inverse absolute negative temperature of the reservoir at lower temperature.

The adiabatic process F$\rightarrow$G

In model II, adiabatic process F$\rightarrow$G is a sudden change in which the system of spin-half particles is detached from the β_3 reservoir and is attached to the β_4 reservoir, see Fig.2.3. The external magnetic field decreases from its value at F to that at G. Due to the sudden change in the external magnetic field, the energy level spacing instantly shifts from Δ_F to Δ_G. There is no heat exchange between the system and the reservoir. The work done, W_{FG}, by the system in $F \rightarrow$G is

$$W_{FG} = p^F(\Delta_F - \Delta_G). \tag{2.33}$$

The quasistatic isothermal processes G$\rightarrow$H

This process begin after the system and the reservoir are first thermalize at G. Once the system is brought in thermal contact with the reservoir at inverse absolute temperature β_4 and relaxes to equilibrium, then it is ready for the next isothermal process

which changes its state from $\{p^G, \Delta_G\}$ to another state, $\{p^H, \Delta_H\}$. Here, the external magnetic field decreases very slowly so that the system remains in equilibrium with the reservoir. During this quasistatic change the occupation probability in the excited state decreases as the system releases heat to the reservoir. The heat released, Q^q_{GH}, in the isothermal process G→H is

$$Q^q_{out} = \frac{1}{\beta_4}[p^E \ln(\frac{1-p^E}{p^E}) - p^G \ln(\frac{1-p^G}{p^G}) + \ln(\frac{1-p^G}{1-p^E})], \tag{2.34}$$

where $p^H = P^E$ used. The corresponding work done on the system is

$$W^q_{GH} = \Delta_H - \Delta_G + \frac{1}{\beta_4} \ln(p^H/p^G). \tag{2.35}$$

2.4.2 The adiabatic process H→E

This is the final process to complete one cycle. When the system reaches a state at H, it is suddenly disconnected from the reservoir at inverse temperature β_4 and then immediately reconnected back to the reservoir at inverse temperature β_3 . This process increases the energy level spacing from Δ_H to Δ_E and thereby returning the system back to the initial state. The work done, $W_{HE}(II)$, on the system during this adiabatic change is simply

$$W_{HE}(II) = p^E(\Delta_E - \Delta_H). \tag{2.36}$$

2.4.3 Net heat absorbed done and efficiency

The system absorbs heat in process E→F and releases it in process G→H. Therefore, the net heat absorbed Q^q_{net} per cycle can be calculated as $Q^q_{net}(II) = Q^q_{EF} + Q^q_{GH}$. Hence,

$$Q^q_{net}(II) = \gamma\beta_3 * Q^q_{in} \tag{2.37}$$

where $\gamma = \beta_3^{-1} - \beta_4^{-1}$, $\beta_3, \beta_4 < 0$ and $|\beta_3| < |\beta_4|$.

The efficiency of the model engine, under quasistatic mode of operation, is the ratio of the net heat absorbed, $Q^q_{net}(II)$ to Q^q_{in}

$$\eta_{II}^{q} = 1 - \frac{\beta_3}{\beta_4}. \tag{2.38}$$

Note that the efficiency expression is a form of Carnot efficiency, η_C.

2.5 Results and discussions

In the discussion of the quasistatic processes and quantities, we deal with processes which involve isothermal processes that enable exchange of energy in the form of work done and heat, and fast changing adiabatic processes which link the isothermal quasistatic processes. We have derived analytic expressions for net heat absorbed, net work done and efficiency of the heat engines. Both the net heat exchange and the work done by the system are functions of the temperatures of the reservoirs and the occupation probability of the excited state of the initial and the final processes. The efficiencies, however, are only functions of the temperatures of the two reservoirs of each model.

In model I, heat is absorbed from the β_1 reservoir and is released to the β_2 reservoir. The net heat absorbed per cycle enable the system to do work. From the ratio of net heat absorbed to the absorbed heat per cycle, we define the quasistatic efficiency η_q for the model and obtain that its efficiency is the Carnot efficiency. From the expression of $\eta_C = 1 - \beta_2/\beta_1$, we computed efficiency of model I as 0.47 ($\beta_1 = 0.8, \beta_2 = 1.5$).

The quasistatic efficiency of model III is also calculated in a very similar way with that of the model I. In the model, the system absorbs heat from the β_5 reservoir and releases it to the β_6 reservoir. As a result, the net heat absorbed enable the system to do work. The quasistatic efficiency, the ratio of the net heat absorbed to the heat absorbed, is only a function of the temperatures of the two reservoirs. In model III, the quasistatic efficiency, η_q is the same as the Carnot efficiency of the model. We determine η_C for the model to be 0.667 ($\beta_5 = 0.5\beta_6 = 1.5$).

In model II in which the engine does work between two reservoirs at negative absolute temperatures, the system absorbs heat from the β_3 reservoir and releases it to the β_4 reservoir. The quasistatic efficiency of this heat engine is also the Carnot efficiency,

$\eta_c = 0.63$ ($\beta_3 = -1.0, \beta_4 = 2.75$).

Chapter 3

Finite-time thermodynamic processes

In this Chapter we describe the finite-time thermodynamic processes and derive the corresponding thermodynamic quantities. Finite-time thermodynamic processes are more realistic non-equilibrium processes that incorporate specifically time in the quantitative description of physical quantities of interest. Net work done, net heat exchange, maximum power (P_{mp}) and the corresponding efficiency at maximum power will be derived.

3.1 The basic blocks for finite-time processes

There are three modes of operations in a finite-time process of our system. The first one is the **adiabatic change** in which the system is detached from the reservoir and subjected to a suddenly changing external magnetic field, for example from point A to a point to the left of point 1, see Fig.3.1; the second one is a process in which the system is left for relaxation. In this process, at a constant external magnetic field, the system is left to relax to equilibrium so that it will be in equilibrium at state 1. In this new equilibrium state, the system would have definite thermodynamic quantities. The third process is attaching the system back to the reservoir. In this process the system exchanges heat with the reservoir for thermalization and finally become in equilibrium with the reservoir. Such consecutive processes complete the finite-time processes. It should be clear that the adiabatic changes, a process in which the system evolves

towards new equilibrium states and the thermalization processes where the system exchanges heat with the reservoir are irreversible processes. However, state A, state 1, and state 2 etc. are all equilibrium states.

In general, the finite-time process involves: detaching the system from a reservoir instantly and adiabatically(changing the level spacing as a result) followed by leaving the system to equilibrate at a constant magnetic field. This is followed by attaching the system back to the reservoir (allowing heat exchange) and wait for thermalization. Concerning the time scales of the processes, the time, τ_a, required to change each adiabatic process (and, hence, time to change the external magnetic field) is much shorter than the time, τ_r, required by the system to relax to its new equilibrium state. The other period is the period for thermalization process where the system is attached to the reservoir, τ_t. The order of these time scales satisfy the relation $\tau_a \ll \tau_r \ll \tau_t$ [17].

3.2 Internal energy, work and heat exchange in finite-time process and the spin-half system

The finite-time process we deal with in this section involves irreversible process. As shown in Eqs.2.6 and 2.7, there are irreversiblity terms accompanying both heat and work done. As the result, entropy generated, $d_{ir}s$, for example (in Model I), in subprocess $A \rightarrow 1$ is

$$d_{ir}s = \frac{\Delta_A - \Delta_1}{T_1} dp^e. \tag{3.1}$$

As it is evident from Fig.3.1, the term $dp^e = p^1 - p^A$ is usually small making the dissipation effect much smaller than the energy exchange in the subprocess. T_1 is the temperature the isolated system attains when it is at equilibrium state 1. Further the relaxation period to equilibrate at 1 is much shorter than the period for thermalization ($1 \rightarrow 2$) after which the system equilibrates at 2. With this assumption, in the remaining calculation of thermodynamic quantities, irreversiblity terms have not been included. As a result, all equations in Chapters 3, 4 and 5 are approximate expressions.

3.3 Finite-time processes (model I)

In the finite-time models, we consider the same working substance as that of quasistatic models. However, the way the external magnetic field varies per process and hence the mechanism of doing work are different.

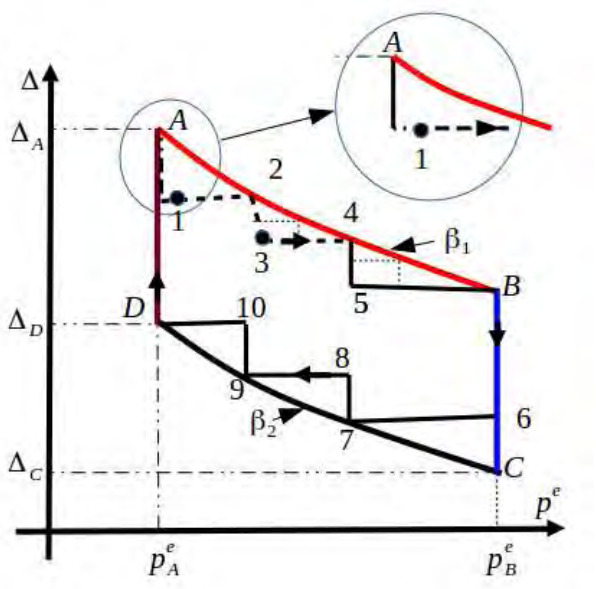

Figure 3.1: Model heat engine working between two reservoirs at distinct positive temperature for finite-time process. Zig-zag segments represent the finite-time process and broken curves represent quasistatic isothermal processes. β_1 is the inverse temperature of the reservoir at higher temperature; whereas β_2 is the inverse temperature of the reservoir at lower temperature.

Fig.3.1 represents the finite-time processes of model I. It is adapted from the quasistatic model presented in Fig.2.2 in a zig-zag way. Same as to the quasistatic model, here also the vertical axis represents the energy level spacing, Δ, while the horizontal axis represents the occupation probability in the excited state. The zig-zag segments show the finite-time processes while the smooth curves show the quasistatic isothermal processes (shown here only for comparison). The inset is the magnification of the finite-time process around the state $\{p^1, \Delta_1\}$. The modes of operations are clearly shown in the plot. The mode of operation at constant occupation probability in the excited state in which the system is detached from the reservoir at state **A** and where its energy level spacing is decreased in a very fast manner from Δ_A to Δ_1. During this sudden change, work of $p^a(\Delta_1 - \Delta_A)$ is done by the system. The second mode is to

wait till the system in isolation attains an equilibrium state at 1 (see Fig.3.1). This will then be followed by attaching the system back to the reservoir and wait until it attains state **2** at constant external field (at Δ_1). During this mode of operation, the system is allowed to exchange heat with the reservoir so that the occupation probability in the excited state changes from p^1 to p^2. As compared to the first two processes, this process should be very slow. During this slow process, $1 \rightarrow 2$, the system absorbs heat of amount $\Delta_2(p^2 - p^1)$. So, Fig.3.1, processes represented by vertical segments: $A \rightarrow 1$, $2 \rightarrow 3$, $4 \rightarrow 5$, $B \rightarrow C$, $C \rightarrow 6$, $7 \rightarrow 8$, $9 \rightarrow 10$ and $D \rightarrow A$ correspond to the first mode of operation-the adiabatic changes. These precesses should immediately be followed by a relaxation of the system to a new equilibrium state before being attached to the reservoir. On the other hand, processes represented by horizontal segments: $1 \rightarrow 2$, $3 \rightarrow 4$, $5 \rightarrow B$, $6 \rightarrow 7$, $8 \rightarrow 9$ and $10 \rightarrow D$ correspond to the third mode of operation-where heat exchange takes place. The entire finite-time process is, therefore, combination of processes adiabatically detaching the system from the reservoir, relaxation of the system to a new equilibrium state and then attaching the system back to the reservoir for thermalization.

The discussion of the following subsections is based on the model diagram given in Fig.3.1. In particular, heat exchange, work done, power and efficiency will be derived. We begin with the zig-zag route $A \rightarrow B$.

3.3.1 The finite-time process A$\rightarrow$ B

In process $A \rightarrow B$, the spin-half system is connected to the β_1 reservoir until it becomes in thermal equilibrium with initial the state $\{p^A, \Delta_A\}$. Then, it is detached from the reservoir and undergoes an adiabatic change in which its level spacing decreases from Δ_A to Δ_1 (process $A \rightarrow 1$). This allows the system to do work $W_{A\rightarrow 1}$ of amount:

$$W_{A\rightarrow 1} = p^A(\Delta_A - \Delta_1). \tag{3.2}$$

The system should wait until it equilibrate at state 1. With the assumption that the energy exchange during this relaxation is small, we did not quantify and include in the calculation of both heat and work. We also follow the same logic for the remaining sections. Immediately after it relaxes to equilibrium, the system is attached back to

the β_1 reservoir. The general expression to calculate the heat exchange is of the type $dQ_{i\to i+1} = \Delta_{i+1}(p^{i+1} - p^i)$. For subprocess 1 →2, $Q_{1\to 2}$, for example, is

$$Q_{1\to 2} = \Delta_2(p^2 - p^1). \tag{3.3}$$

The absorbed heat, in turn, increases the occupation probability from p^1 to p^2 (process $1 \to 2$). The total heat absorbed during the finite-time process $A \to B$ (for n=3 is the number of subdivisions used), Q^f_{AB}, is then equal to the sum of the heat absorbed during the subprocesses 1→2, 3→4 and 5→ B. Hence,

$$Q^f_{A\to B} = \Delta_B p^B - \Delta_A p^A + \Delta(p^A + p^2 + p^4), \quad where \;\; p^1 \approx P^A \tag{3.4}$$

and the corresponding work done by the engine is

$$W^f_{AB} = -\Delta(p^A + p^2 + p^4), \tag{3.5}$$

where $\Delta = (\Delta_A - \Delta_B)/n$, in Fig.3.1, n=3. Note that, in the finite-time of our interest, Q^f_{AB} is positive, whereas the work done by the system is negative since the system looses its internal energy.

3.3.2 The adiabatic process B→C

When the system reaches state B, $\{p^B, \Delta_B\}$, it is detached from the β_1 reservoir and instantaneously connected to the β_2 reservoir. Simultaneously, the level spacing of the system instantly changes from Δ_B to Δ_C. However, the occupation probability of the system remains unchanged (i.e, $p^B = p^C$). It is important to note that there is no heat exchange between the system and the reservoirs during this adiabatic change. The amount of work done by the system, $W_{B\to C}$, is

$$W_{B\to C} = p^B(\Delta_C - \Delta_B). \tag{3.6}$$

3.3.3 The finite-time process C→ D

This is a process in which the occupation probability of the spin-half particles in the excited state decreases. Just after the adiabatic process B→C is completed, the system is left to exchange heat with the β_2 reservoir with which thermal equilibrium should

be reached before the next adiabatic change commences. By increasing the external magnetic field adiabatically, it is possible to increase the energy level of the system from Δ_C to Δ_6. At the same energy level spacing (Δ_6), the system has to relax to an equilibrium state. After relaxation, it is ready to be attached back to the β_2 reservoir. In the same manner, processes 6→7, 8→9 and 10→D continue while intermittently attaching to the β_2 reservoir in between. The finite-time heat released Q^f_{CD} by the system in process C→D (see Fig. 3.1) is thus

$$Q^f_{C\to D} = \Delta_D p^D - \Delta_C p^C - \Delta^{'}(p^C + p^7 + p^8). \tag{3.7}$$

Once again the dissipation term due to irreversiblity is ignored with the same reason given in the previous subsection. So,the work done on the system along the path $C \to D$, which is positive, is

$$W^f_{CD} = \Delta'(p^C + p^7 + p^8), \tag{3.8}$$

where $\Delta' = (\Delta_D - \Delta_C)/n$, n=3 in Eq.(3.7).

3.3.4 The adiabatic process D→A

When the system reaches state D, $\{p^D, \Delta_D\}$, it is detached from the β_2 reservoir and is instantaneously reconnected back to the β_1 reservoir. Simultaneously, the energy level spacing of the system changes from Δ_D to Δ_A without affecting the distribution of the spin-half system, i.e, $p^D = p^A$. The amount of work done on the system $W_{D\to A}$ in this subprocess is

$$W_{D\to A} = p^A(\Delta_A - \Delta_D). \tag{3.9}$$

In general, the system begins from the (initial) state $\{p^A, \Delta_A\}$ and returns back to the same state in one cycle. Note that when the stairs describing the finite-time process is infinitesimally small (i.e., when large number of subdivisions is used), the finite-time process approaches the quasistatic process. A magnification of the state around state 2 in Fig.3.1 is shown in the inset and this is to make clear how the finite-time process approaches the corresponding quasistatic process when large number of subdivisions is used.

3.3.5 Net heat exchange and net work done per cycle (model I)

The system absorbs heat, $Q^f_{in}(I)$, in process A→B and releases heat, $Q^f_{out}(I)$, in process C→D. So, the heat absorbed and released, respectively, are

$$Q^f_{in}(I) = (\Delta_B p^B - \Delta_A p^A) + \Delta(p^A + p^2 + p^4), \tag{3.10}$$

and

$$Q^f_{out}(I) = (\Delta_D p^D - \Delta_C p^C) - \Delta'(p^C + p^7 + p^9). \tag{3.11}$$

And the net heat absorbed per cycle, $Q^f_{net}(I)$, is the sum of the heat exchange in the process A→B and C→D so that

$$Q^f_{net}(I) = (\Delta_B p^B - \Delta_A p^A)(1 - \Delta_C/\Delta_B) + (\Delta p^A - \Delta' p^C) + (\Delta - \Delta')(p^2 + P^4). \tag{3.12}$$

Work is done by the engine during the processes A→ B →C. The work done by the system on the reservoir, W^f_{sr}, is

$$W^f_{sr}(I) = (\Delta_C - \Delta_B)p^B - \Delta(p^A + p^2 + P^4), \tag{3.13}$$

whereas the work done on the system, W^f_{rs}, is the work done in the processes C→ D →A. Hence,

$$W^f_{rs}(I) = (\Delta_A - \Delta_D)p^A + \Delta'(p^C + p^7 + P^9). \tag{3.14}$$

The net work done, $W^f_{net}(I) = W^f_{sr}(I) + W^f_{rs}(I)$, is then

$$W^f_{net}(I) = (\Delta_A p^A - \Delta_B p^B)(1 - \Delta_C/\Delta_B) + (\Delta' p^C - \Delta p^A) + (\Delta' - \Delta)(p^2 + P^4). \tag{3.15}$$

3.3.6 The finite-time power and efficiency (model I)

Power in a heat engine which performs a task in a cycle is the amount of work done per unit time. So, to derive the expression of power, it is important to find the time duration taken by each subprocesses and its relation to the number of subdivisions used to study the finite-time process. Indeed, when the number of subdivisions n is large (and

approaches infinity), the finite-time processes approach their corresponding quasistatic isothermal processes. So, the quasistatic limit (infinite time) corresponds to finite-time process, where the number of subdivisions is infinitely large (n$\rightarrow \infty$). Small number of subdivisions would mean fast process (as n is Small, the time to complete a process is also small and the process takes finite time). We can, therefore, assume that time to complete a process is proportional to the number of subdivisions. This assumption has also been used earlier by M. Alemye [25] and W. Chegeno [26] in their study of a model quantum heat engine working in a finite-time. Therefore, we take the assumption $t \propto n$.

In the three basic modes of operations (Sec.3.1.), the adiabatic process in which the system is detached from a reservoir and the external magnetic field is instantly changed by a finite amount and in the process where the system relaxes to an equilibrium state before attaching to a reservoir, no time elapses are assumed. However, in the thermalization process where the system is brought in contact with the reservoir until it equilibrate with it, there is time elapse. Therefore, the time taken to change on the external magnetic field to undergo adiabatic changes and the relaxation time are much smaller than than the time required by the system to equilibrate with the reservoirs. The period of a cycle, the total time taken to complete one cycle, is simply the sum of the time elapsed during the equilibration processes.

Thus in model I, for example, $t = n$(to under go at constant occupation probability in the excited state in process A$\rightarrow$B) or n(to under go at constant occupation probability in the excited state in process C$\rightarrow$D). This implies $n = t$. With these and the net heat absorbed by the system, we can write the expression of power for model I, $P_I(t)$, as

$$P_I(t) = -\frac{W^f_{net}(I)}{t}. \tag{3.16}$$

The negative sign only indicates that the work is done by the engine. Using Eq.3.15, the expression of power for model I can be written as

$$P_I(t) = \frac{M}{t} - \frac{L}{t^2}, \tag{3.17}$$

where $M = (\Delta_B p^B - \Delta_A p^A)(1 - \Delta_C/\Delta_B)$ and $L = (\Delta_D - \Delta_C)p^C - (\Delta_A - \Delta_B)p^A + (\Delta_D + \Delta_B - \Delta_C - \Delta_A)(p^2 + p^4)$,$\Delta = (\Delta_A - \Delta_B)/n$, $\Delta' = (\Delta_D - \Delta_C)/n$ and $t \propto n$.

The efficiency of model I, $\eta_I(t)$, is the ratio of net heat absorbed (net work done) by the engine ($Q^f_{net}(I)$), to the heat absorbed by the engine , Q^f_{AB}. Hence,

$$\eta_I(t) = \frac{M - \frac{L}{t}}{J + \frac{K}{t}} = 1 + \frac{\Delta_D p^D - \Delta_C p^C - \Delta'(p^C + p^7 + p^9)}{\Delta_B p^B - \Delta_A p^A + \Delta(p^A + p^1 + p^2)}, \tag{3.18}$$

where $J = \Delta_B p^B - \Delta_A p^A$ and $K = (\Delta_A - \Delta_B)(p^A + p^2 + p^4)$. In the very long period of operation, the efficiency η^q of model I would reduce to a simple expression of either $1 - \Delta_C/\Delta_B$ or $1 - \Delta_D/\Delta_A$ both of which are simply the Carnot efficiency of the model.

In the finite-time processes of model I, the system absorbs heat from the β_1 reservoir and does work in $A \to B$. By the time the system reaches state B, the internal energy U of the system decreases from U_A to U_B. In the adiabatic process $B \to C$, in which the system is detached form the β_1 reservoir and attached to the β_2 reservoir, the system has done additional work done causing its internal energy to further decrease from U_B to U_C. So, the decrease in internal energy of the system from A to C appears as the work done by the system in the finite time process $A \to B \to C$. The system releases heat in the finite-time subprocess $C \to D$. In this process, work is done on the system thereby increasing the internal energy of the system from its U_C to U_D. The adiabatic process $D \to A$, further increases the internal energy of the system U_D to U_A and returns the system to the original state A.

3.4 The finite-time process (model III)

This model engine is similar to the model engine presented in Sec.3.3. The notable differences are the direction of the external magnetic field to which the system of spin-half particles is subjected to and the range of values of the occupation probability p^e in the excited state. In the former case, $p^e < 0.5$; whereas in this case $p^e > 0.5$. The model engine absorbs heat as the occupation probability in the excited state decreases and releases heat as p^e increases. Other than these, both have similar modes of operation.

Fig.3.2 represents the finite-time process of model III and is adapted from the quasistatic model engine presented in Fig.2.1. The zig-zag (broken) segments show the

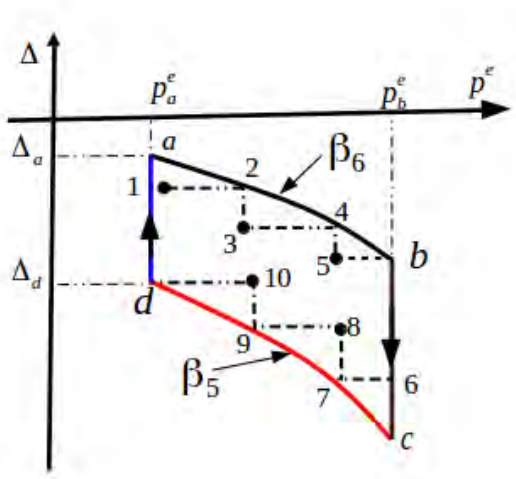

Figure 3.2: Model heat engine working between two positive temperatures for finite-time process. Broken segments represent the finite-time process. Smooth curves represent quasistatic isothermal processes. β_5 is the inverse temperature of the reservoir at higher temperature; whereas β_6 is the inverse temperature of the reservoir at lower temperature.

finite-time processes. The three basic building blocks of a finite-time process presented in Sec.3.2 also apply here. Though, for simplicity, it is better to start the process from state $\{p^c, \Delta_c\}$ and then move the system towards the state $\{p^d, \Delta_d\}$ during which the system absorbs heat from the reservoir, however, we begin from state $\{p^a, \Delta_a\}$ to adapt the previous scenario.

3.4.1 The finite-time process a→ b

In the finite-time process $a \to b$, the spin-half system is initially connected to the β_6 reservoir until it becomes in thermal equilibrium with the initial state $\{p^a, \Delta_a\}$ at point **a**. Then, it is detached from the reservoir and undergoes an adiabatic change in which its level spacing decreases from Δ_a to Δ_1 (process $a \to 1$). This allows the system to do work $W_{a\to 1}$ of amount

$$W_{a\to 1} = p^a(\Delta_1 - \Delta_a). \tag{3.19}$$

Before attaching the system with the β_6 reservoir, it is left to relax and find a new equilibrium state around (to the right and close to point 1) state 1. Similar to model I, assuming dissipation effects small, irreversible heat and work have not been taken into account.

The next process is to attach the system to the reservoir until it equilibrates with the β_6 reservoir. In this equilibration process, $1 \rightarrow 2$, there is heat release, $Q^f_{1\rightarrow 2}$ from the system to the reservoir of amount

$$Q^f_{1\rightarrow 2} = \Delta_1(p^2 - p^1). \tag{3.20}$$

Note that Δ_1 is negative so that $Q^f_{1\rightarrow 2} < 0$, signifying that our system looses heat.Similarly in the subprocesses $1 \rightarrow 2$, $3 \rightarrow 4$ and $5 \rightarrow$b the system looses heat to the reservoir. The heat released in the finite-time process $a \rightarrow$b, Q^f_{ab}, is, therefore, the sum of the heat released in these subprocesses. Hence,

$$Q^f_{ab} = \Delta_b p^b - \Delta_a p^a + \Delta^{"}(p^a + p^2 + p^4). \tag{3.21}$$

where $\Delta^{"} = (\Delta_a - \Delta_b)/n$, n=3. The corresponding finite-time work done by the system in the process $a \rightarrow b$, W^f_{ab}, is the sum of the work done by the system in the subprocesses: $a \rightarrow 1$, $2 \rightarrow 3$ and $4 \rightarrow 5$.

$$W^f_{ab} = -\Delta^{"}(p^a + p^2 + p^4), \tag{3.22}$$

where $\Delta^{"} = (\Delta_a - \Delta_b)/n$, n in Eqs.

3.4.2 The adiabatic process b→c

This adiabatic process is a process in which the system is detached from the β_6 reservoir and then attached to the β_5 reservoir instantaneously. Only energy level spacing changes by this subprocess; as a result, there is only work done, W^f_{bc}, of amount

$$W^f_{bc} = p^b(\Delta_c - \Delta_b) \tag{3.23}$$

is done by the system.

3.4.3 The finite-time process c→ d

This process takes place after the adiabatic process b→c and the system equilibrate with the β_5 reservoir. It is a process in which the occupation probability of the spin-half particles in the excited state generally decreases. This finite-time process begins

with detaching the system from the β_5 reservoir and then increasing the energy level spacing from Δ_c to Δ_6 during which work of amount, $W^f_{c\to 6} = p^c(\Delta_6 - \Delta_c)$, is done on the system. After the system is subjected to an adiabatic change and its levels spacing increases (from Δ_c to Δ_6), the system should be let free to equilibrate. Then the system is attached back to the β_5 reservoir so that it will be in equilibrium with the reservoir. So, work is done on the system in the subprocesses $c \to 6$, $7 \to 8$ and $9 \to 10$. On the other hand, heat is absorbed in the subprocesses $6 \to 7$, $8 \to 9$ and $10 \to$D. The work done, W^f_{cd}, on the system in the finite-time process is thus

$$W^f_{c\to d} = \Delta^t(p^c + p^7 + p^9), \tag{3.24}$$

and the heat absorbed in finite-time process c$\to$d, Q^f_{cd}, is, see Fig. 3.2,

$$Q^f_{c\to d} = \Delta_d p^d - \Delta_c p^c - \Delta^t(p^c + p^7 + p^9), \tag{3.25}$$

where $\Delta^t = (\Delta_d - \Delta_c)/n > 0$, n is as defined in Sec.3.2.1.

3.4.4 The adiabatic process d$\to$a

This is the final process to complete one cycle. Once the system equilibrates at the state D, $\{p^d, \Delta_d\}$, it is detached from the β_5 reservoir and suddenly attached back to the β_6 reservoir. Instantly, the energy level spacing of the system is made change from Δ_d to Δ_a without affecting the distribution of the spin-half system, i.e, $p^d = p^a$. The amount of work done on the system, $W^f_{d\to a}$, in this subprocess is then

$$W_{d\to a} = p^a(\Delta_a - \Delta_d). \tag{3.26}$$

3.4.5 Net work done and net heat exchange per cycle (model III)

The system does work in the process a$\to$ b $\to$c. The amount of work done by the system in this process, W^f_{abc}, is

$$W^f_{abc} = (\Delta_c p^c - \Delta_b p^b) - \Delta"(p^a + p^2 + p^4), \tag{3.27}$$

whereas work done on the system in the process c$\to$ d $\to$a, W^f_{cda}, is

$$W^f_{cda}(III) = (\Delta_a p^a - \Delta_d p^d) + \Delta^t(p^c + p^7 + p^9). \tag{3.28}$$

The net work done per cycle, $W^f_{net}(III)$, is the sum of the work done by the system, W^f_{abc}, and the work done on the system, W^f_{cda},:

$$W^f_{net}(III) = (\Delta_c p^c - \Delta_d p^d)(1 - \frac{\Delta_a}{\Delta_D}) + \frac{L^{'}}{t}. \tag{3.29}$$

where $L^{'} = (\Delta_d - \Delta_c)p^c - (\Delta_a - \Delta_b)p^a + (\Delta_d + \Delta_b - \Delta_c - \Delta_a)(p^2 + p^4)$. The heat absorbed, Q_{in}, takes place in process c→d of Eq.3.25; whereas an amount of heat, $Q_{out}(III)$, is released in process a→b of Eq.3.21. Hence, the net heat exchanged per cycle of the model is

$$Q^f_{net}(III) = -W^f_{net}(III) = (\Delta_d p^d - \Delta_c p^c)\eta_C + \Delta^{"}(p^a + p^2 + p^4) - \Delta^t(p^c + p^7 + p^9), \tag{3.30}$$

where $\eta_C = 1 - \Delta_a/\Delta_d$ and $\Delta_a/\Delta_d = \Delta_b/\Delta_c$.

3.4.6 Finite-time power and efficiency (model III)

Similar to the explanations given above for model I, power for model III, $P_{III}(t)$, is simply net work done per unit time (per cycle) and is given as

$$P_{III}(t) = \frac{Q^f_{net}(III)}{t}. \tag{3.31}$$

Using Eq.(3.28) in Eq.(3.30), we get the expression for $P_{III}(t)$ to be

$$P_{III}(t) = \frac{M^{'}}{t} - \frac{L^{'}}{t^2}, \tag{3.32}$$

where $M^{'} = (\Delta_d p^d - \Delta_c p^c)(1 - \Delta_a/\Delta_d)$.

Efficiency of model III, $\eta_{III}(t)$, is the ratio of net heat absorbed to the heat absorbed by the system in subprocess $c \to d$. Hence,

$$\eta_{III}(t) = \frac{M^{'}t - L^{'}}{J^{'}t - K^{'}} \tag{3.33}$$

where $J^{'} = \Delta_d p^d - \Delta_c p^c$ and $K^{'} = (\Delta_d - \Delta_c)(p^c + p^7 + p^9)$.

3.5 Finite-time process (model II)

This is a process which takes place between a system of spin-half particles and two reservoirs at negative absolute temperatures. In this process, the occupation probability of the excited state is at least greater than or equal to 0.5. With the aid of external magnetic field and heat exchange between the system and the reservoirs, the tree modes of operation should sequentially complete a cycle. During such changes, there are heat exchange and wok done on(by) the system. In particular, in processes: 1→2, 3→4 and 5→F, the system absorbs heat from the reservoir (see Fig.3.3). In processes E→1, 2→ 3, 4→5 and H→E, work is done by the system. In processes: F→G, G→6, 7→8 and 9→10 work is done by the system. Processes: 6→7, 8→ 9 and 10→H, the system releases heat. It is these finite number of alternate adiabatic and changes at constant probability that completes the finite-time process E→ $F \rightarrow G \rightarrow H \rightarrow$E, see Fig.3.3

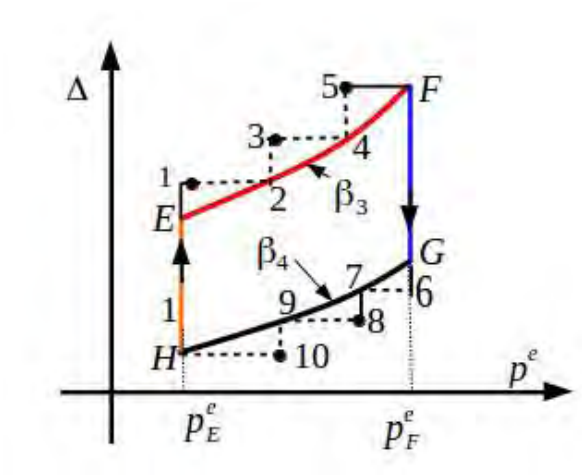

Figure 3.3: Model heat engine working between two negative absolute temperatures for finite-time process. Broken segments represent the finite-time process. Smooth curves represent quasistatic isothermal processes. β_3 is an inverse negative temperature of the reservoir at lower temperature; whereas β_4 is the inverse negative temperature of the reservoir at higher temperature.

3.5.1 Finite-time process $E \rightarrow$ F

As far as the the process moves clock-wise, one can start from any equilibrium state. Thus, let us start the process from state E with coordinate point $\{p_E, \Delta_E\}$ at the β_3 inverse temperature . To start the process, we detach the system from the reservoir and

suddenly increase the external magnetic field so as to change its energy level spacing from Δ_E to Δ_1. In this process, there is only work done by the system (of amount $W_{E\to 1} = p^E(\Delta_1 - \Delta_E)$; no change in occupation probability. Then the system should attain a new equilibrium state before attaching it back to the β_3 reservoir. What follows is a process at constant external field which allows the system to absorb heat, of amount $Q_{1\to 2} = \Delta_1(p^2 - p^1)$, from the reservoir. Similar alternate operation of detach, wait for relaxation and attach to the reservoir will successfully take the system through the zig-zag up to F. Heat absorption takes place in this finite-time subprocesses (the horizontal segments) of $E \to$F. The heat absorbed, Q^f_{EF}, in E$\to$F is sum of absorbed heat in the horizontal segments and its sum becomes

$$Q^f_{EF} = \Delta_F p^F - \Delta_E p^E - \Delta^r(p^E + p^2 + p^4), \tag{3.34}$$

On the other hand, work is done by the system in the finite-time subprocesses(in the vertical segments) of E$\to$F. Thus, the work done, W^f_{EF}, is the sum of the work done in the vertical segments:

$$W^f_{EF} = \Delta^r(p^E + p^2 + p^4), \tag{3.35}$$

where, both in Eqs.3.34 and 3.35, $\Delta^r = (\Delta_F - \Delta_E)/n$ and n is the number of subdivisions, n being equal to 3 in this case.

3.5.2 Adiabatic process F$\to$ G

This is a process in which our system is detached from the β_3 reservoir and is attached to the β_4 reservoir. The work done by the system, W^f_{FG}, in this adiabatic process is

$$W^f_{FG} = p^F(\Delta_G - \Delta_F). \tag{3.36}$$

3.5.3 Finite-time process G$\to$ H

In this process, the occupation probability in the excited state generally decreases as we go from p^G to p^H. After the system is thermalized with the β_4 reservoir at state G, $\{p^G, \Delta_G\}$, it is suddenly brought to $\{p^6, \Delta_6\}$ by decreasing the external magnetic field and then left for relaxation after which it is attached back the reservoir with which it

exchanges heat. Similar to the previous processes, the total heat released during the process G→H then can be added together to give Q^f_{GH} as

$$Q^f_{GH} = \Delta_H p^H - \Delta_G p^G + \Delta^s(p^G + p^7 + p^9), \tag{3.37}$$

whereas the work done by the system, W^f_{GH}, in this finite time process becomes

$$W^f_{GH} = -\Delta^s(p^G + p^7 + p^9), \tag{3.38}$$

where, $\Delta^s = (\Delta_G - \Delta_H)/n$ and $n = 3$, for example in Fig.3.3, is the number of subdivisions and is equal to 3 in this case also.

3.5.4 Adiabatic process H→ E

This change is the final process to complete one cycle. It can be carried out by disconnecting the system from the β_4 reservoir and immediately attaching it to the β_3 reservoir whereby the energy level spacing of the system increase from Δ_H to Δ_E . This would finally bring the system to the initial state. The work done on the system in this adiabatic change is thus

$$W^f_{HE} = p^E(\Delta_E - \Delta_H). \tag{3.39}$$

3.5.5 Net heat exchange and net work done per cycle of model II

In this section, we summarize the net heat and net work done by model II. This model is different from the models presented in the last two section due to the fact that it performs a task between two reservoirs which are at negative absolute temperatures. In a cycle, the net heat exchanged by the model engine during the finite-time process, is the sum of the heat absorbed in the process E→F, Eq.3.34 and that released in the process G→H, Eq.3.37:

$$Q^f_{net}(II) = \Delta_F p^F(1-\frac{\Delta_G}{\Delta_F}) - \Delta_E p^E(1-\frac{\Delta_H}{\Delta_E}) + \Delta^s(p^G+p^7+p^9) - \Delta^r(p^E+p^2+p^4) \tag{3.40}$$

The net work done by the system is the same as the net heat exchange by the system but it is negative.

3.5.6 Finite-time power and efficiency of model II

Since the time taken to switch on the external field which drive the adiabatic changes and the relaxation time for the system are assumed to be much faster than the time taken to undergo equilibration process of the system with the reservoirs, time elapsed during all the adiabatic changes and the relaxation processes are considered to be negligible and hence are not accounted to in the calculation of period. And consequently, the period of a cycle, the total time taken to complete one cycle does not include the periods for these two changes.

Thus, similar to the two models presented in Sec.3.3. and 3.4, in model II also , $t = n$(to under go finite-time process E→F) or n(to under go finite-time process G→H). This implies $n = t$. Using this concept and the net heat absorbed, we can write the expression for power and efficiency of model II, $P_{II}(t)$, as

$$P_{II}(t) = \frac{Q^f_{net}(II)}{t}, \tag{3.41}$$

In a simple form:

$$P_{II}(t) = \frac{R}{t} - \frac{V}{t^2}, \tag{3.42}$$

where $R = (\Delta_F p^F - \Delta_E p^E)\eta_C$, $V = (\Delta_F - \Delta_E)(p^E + p^2 + p^4) - (\Delta_G - \Delta_H)(p^F + p^7 + p^9)$ and $\eta_C = 1 - \Delta_G/\Delta_F = 1 - \Delta_H/\Delta_E$.

And efficiency of model II, $\eta_{II}(t)$, the ratio of net heat absorbed to the heat absorbed by the system, can be written as

$$\eta_{II}(t) = \frac{Rt - V}{rt - v} \tag{3.43}$$

where $r = \Delta_F p^F - \Delta_E p^E$ and $v = (\Delta_F - \Delta_E)(p^E + p^2 + p^4)$

In this subsection, we have described the finite-time process and derived the expressions for the net heat absorbed, power and efficiency of model II.

3.6 Thermodynamic quantities at maximum power

In this section, we explore the maximum power and efficiency at maximum power for the models. Maximum power mode of operation in heat engine refers to the operation of the engine in which task is accomplished and work is extracted from the system in such a finite-time of operation enabling the engine to attain maximum power. Since power, both in the shortest and longest (quasistatic limit) times of operation, is zero, maximum power working condition, in which task is accomplished at finite time, is important for a heat engine. Thus, in the subsequent subsections, we explore power and other finite-time quantities such as efficiency and period under the maximum power working conditions.

3.6.1 Maximum power (P_{mp}) and efficiency at maximum power (η_{mp})

Taking an Atwood machine as a mechanical energy converter, six decades ago, early study of efficiency at maximum power was conducted by Odum and Pinkerton [27]. However, as a finite-time thermodynamic quantity, maximum power mode of operation of heat engine has been studied two decades latter by Curzon and Ahlborn [14]. Starting from some simple assumptions, they have obtained an expression for the efficiency at maximum power (EMP) as $\eta_{mp} = 1 - \sqrt{T_c/T_h}$ for a heat engine operating between two distinct positive temperatures T_h (hot) and T_c (cold) where $T_h > T_c$. Since then many model energy converters have been studied and their efficiencies at maximum power (and maximum power) have been reported, [27, 28, 29]. These works show that it is possible to maximize power of heat engines to accomplish tasks in a short enough finite time. But such a working condition usually does not give good performance for heat engine due to poor corresponding efficiency.

3.6.2 P_{mp} and η_{mp} of model I

In order to find the maximum power P_{mp} of the model engine, the expression for power, P(t) from Eq.3.17 should be subjected to the condition:

$$\frac{dP_I(t)}{dt}|_{t=\tau_{mp}} = 0, \tag{3.44}$$

where $P_{mp} = P_I(\tau_{mp})$ and τ_{mp} is the period at which the power attains its maximum value. Therefore, the period at which the engine attains its maximum power is

$$\tau_{mp} = \frac{2L}{M}, \quad and \tag{3.45}$$

$$P_{Imp} = \frac{M^2}{4L} \tag{3.46}$$

Efficiency of the model engine at maximum power, $\eta_I(\tau_{mp}) = \eta_{Imp}$, can hence be simplified to give

$$\eta_{Imp} = \frac{\eta_C}{2(1 + \frac{1}{2}z\eta_C)}, \tag{3.47}$$

where the ratio of K and L, $z = \frac{(\Delta_A - \Delta_B)(p^A + p^2 + p^4 + ...)}{(\Delta_D - \Delta_C)(p^C + p^7 + p^9 + ...) - (\Delta_A - \Delta_B)(p^A + p^2 + p^4 + ...)}$.

3.6.3 P_{mp} and η_{mp} of model III

Similar to model I, the maximum power P_{mp} of model III could be computed from

$$\frac{dP_{III}(t)}{dt}|_{t=\tau_{mp}} = 0, \tag{3.48}$$

And this is satisfied when

$$\tau_{mp} = \frac{2L^{'}}{M^{'}}. \tag{3.49}$$

Hence, the maximum power and efficiency at maximum power for the model, respectively, are

$$P_{mp} = \frac{M'^2}{4L^{'}}, \tag{3.50}$$

$$\eta_{mp} = \frac{\eta_C}{2(1 - \frac{1}{2}x\eta_C)}, \tag{3.51}$$

where $x = \frac{K^{'}}{L^{'}}$.

3.6.4 P_{mp} and η_{mp} of model II

In order to find the the maximum power for the model, we need to subject Eq.3.42 to the condition:

$$\frac{dP_{II}(t)}{dt}|_{t=\tau_{mp}} = 0. \tag{3.52}$$

The period at which this condition is fulfilled is $\tau_{mp} = 2V/R$. The corresponding maximum power, $P_{mp}(II)$ is

$$P_{mp}(II) = \frac{R^2}{4V}. \tag{3.53}$$

One can easily find the efficiency of the system at the maximum power for model II from $\eta_{II}(\tau_{mp}) = \eta_{II}(mp)$ and get

$$\eta_{mp}(II) = \frac{1}{2}\frac{\eta_C}{(1 - \frac{\eta_C}{2}\chi)}, \tag{3.54}$$

where $\chi = \frac{v}{V}$.

3.7 Results and discussions

The results of the thermodynamics quantities are generated with Fortran programming As demonstrated in Fig.3.4, the system takes time to absorb heat that is large enough to yield net work done. As a consequence, power start at $\tau = 4$ and rapidly increase until it reach its peak value at $\tau = 7$. Once the maximum power(P_{mp}) is reached, however, power decreases continually and loses half of its value in the next two fold of the period required to attain P_{mp}. In the very long period limit ($\tau \rightarrow$ large), where the system takes longer and longer period to do some finite work, power approaches the quasistatic limit, wherein, it eventually becomes vanishingly small.

At the beginning, the system takes time to absorb heat and, therefore, for some time interval, the net work done and consequently power is negligible. After $\tau = 4$, because of the increment in the net absorb heat and therefore of the increment of the net work done, power increase continually. However, as period τ becomes longer and longer (but $\tau \leq \tau_{mp}$), its effect becomes so significant that power is unable to further increase

with an increase in the net work done, and this leads to the existence of a maximum power(P_{mp}) at a particular period $\tau = \tau_{mp}$ (see Fig.5.1). Beyond this point, due to the longer time taken by the system to do some finite work, power decreases continually and approaches the quasistatic limit.

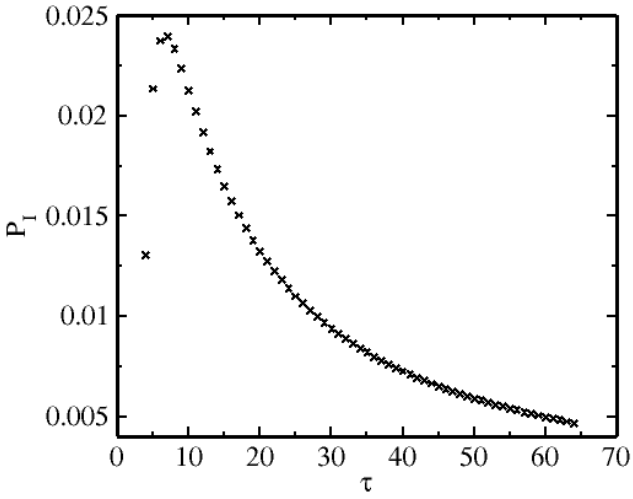

Figure 3.4: Plt of power versus period for model I. $\beta_1 = 0.80, \beta_2 = 1.5, p^A = 0.02$ and $p^B = 0.34$.

Figure 3.5 shows efficiency versus period of the heat engine of model I. Efficiency first grows exponentially at early periods and then slow down after $\tau = 15$ period unit. The observed sharp increases are the combined effect of the work done by the system and the work done on the system: both of them (see Fig.3.1, zig-zag segment $A \rightarrow$B) and the decrease in the work done on the system (see the same Fig, zig-zag segment $C \rightarrow$ D) have contributed to the increment of the net work done, which in turn increases the efficiency of the system. Hence, with increment in period the system becomes more and more efficient and approaches the quasistatic limit in the longer periods.

The efficiency of the system becomes positive after the system begins doing net work ($\tau \geq 4$). Because the net work done by the system increases with period in the first about 16 units of period, efficiency of the system increases very rapidly with period and then slow down the increasing rate. Eventually, in the very longer period (60 unit and above), it becomes the quasistatic efficiency (0.45) which approaches the Carnot efficiency (0.47) for the model and hardly increases any more.

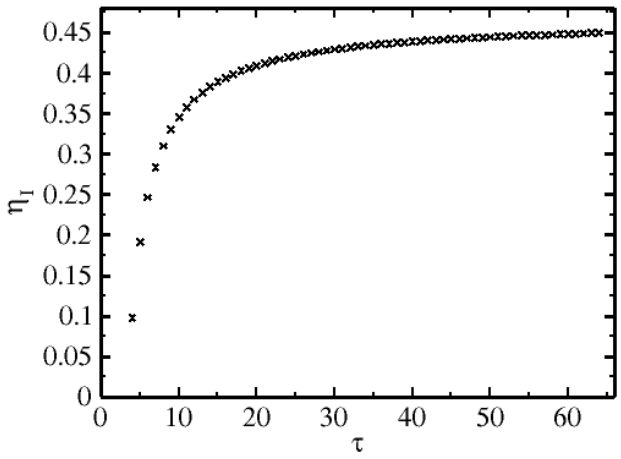

Figure 3.5: Plot of efficiency versus period for model I. $\beta_1 = 0.80, \beta_2 = 1.5, p^A = 0.02$ and $p^B = 0.34$.

Fig.3.6 shows power versus period for the finite-time process of model III. As it is depicted in the Fig., the system takes some time to absorb net heat from the reservoirs. So, both power and net work done are essentially small during those periods. Power, which depends on the net work done and period, increases as the net work done by the system increases. This is because period is not long enough to influence the power. So, the dominant factor, when period is short, is the net work done. Due to this fact, power increases with an increase in the net work done. However, as period becomes longer and longer, power has come to a point where any further increase in net work done does not increase it any more and reaches its maximum power $P_{mp}(III)$ at a particular period, τ_{mp}, see Fig.5.3. Beyond this, period dominates power. As a result we observe a decrease in power as the period increases further.

The system begins operating as a heat engine after period becomes 5 units. The power of the system increase until it attains the maximum power,P_{mp}, at $t = 9$. Once P_{mp} is attained, it decreases very slowly. In the long period of operation, the power of the system approaches the vanishingly quasistatic power.

Fig.3.7 shows the plot of efficiency versus period for model III. It is observe that the system takes initially some time before doing some net work done. Once it starts doing net work done, efficiency sharply increases as the work done by the system increase. The implication is that the **net** work done increase more than the work done by the

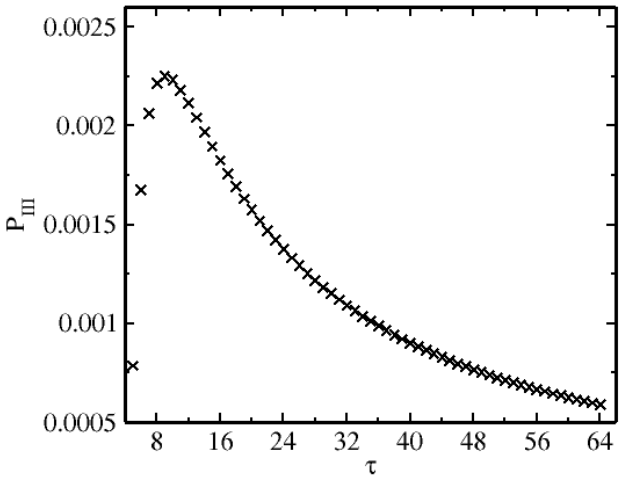

Figure 3.6: Plot of power versus period for model III.$\beta_5 = 0.50, \beta_6 = 1.5, p^d = 0.54$ and $p^c = 0.80$.

system. The increase from the work done by the system (see Fig.3.2, zig-zag segment $c \rightarrow$ d) and the decrease of the work done on the system (see the same Fig, zig-zag segment $a \rightarrow$b) have both contributed to the increment of the net work done-which in turn increases the efficiency of the system. So, with increment in period the system becomes more and more efficient. However, once it approaches the quasistatic efficiency, in the very long period, it hardly increase.

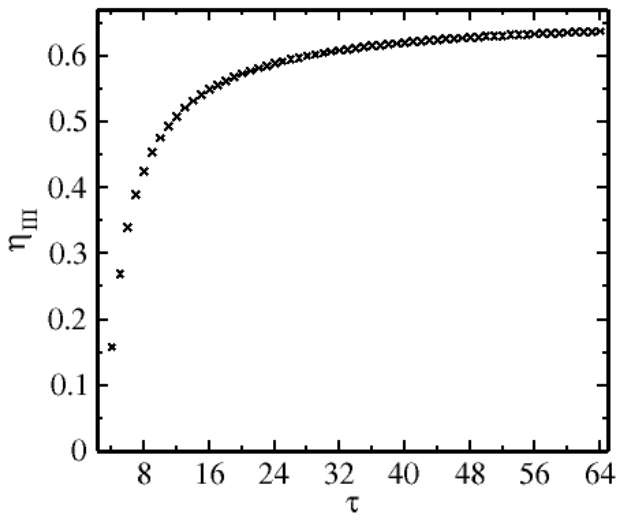

Figure 3.7: Plot of efficiency versus period for model III. $\beta_5 = 0.50, \beta_6 = 1.5, p^d = 0.54$ and $p^c = 0.8$.

From period point of view, we observe that efficiency increases sharply in the first 20 period units, see Fig.5.4. For about the next 10 period unit, efficiency increases gently with period and then tends to behave steadily. After 60 period units, the efficiency of the system increases so slowly that no significant change is observed.

Fig.3.8 shows power versus period of model II. In this model as well, power depends on both net work done and period. Since it is dominated by net work done in the small period values, we observe an increase in power as the net work done increases. However, as period τ becomes longer and longer (but $\tau \leq \tau_{mp}$), power does not simply increase with an increase in net work done rather period also becomes so significant that power is unable to further increase with an increase in the net work done. At a particular value of period $\tau = \tau_{mp}$, further increase in power stops. Beyond this point, power is dominated by period and decrease as period increases. As the system, then, takes longer and longer period to do some finite work, power is approaching the quasistatic limit, wherein, it eventually becomes vanishingly small.

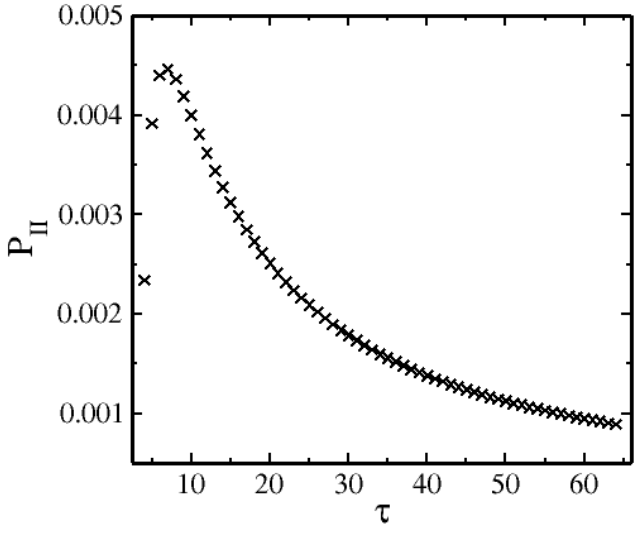

Figure 3.8: Plot of power versus period for model II. $\beta_3 = -1.0, \beta_4 = -2.75, p^E = 0.64$ and $p^F = 0.74$.

In general, the power of this model initially increases as period increase from $\tau = 4$ to $\tau_{mp} = 8$, see Fig.5.5. For longer periods than τ_{mp}, power essentially decreases. By the

time when period is 40 units, power has decreased to 31% of its p_{mp}. At the end when period is 64 units, power has dropped to less than 20% of its peak value. For curiosity, we have checked that when period is 120 units, power is only 10% of its maximum power.

Fig.3.9 depicts efficiency versus period for model II. The efficiency of model II increases similar to the other two models. It naturally approaches the quasistatic efficiency as the period of operation is very long. The calculated quasistatic efficiency, from Eq.3.43 is 0.577. The the efficiency of this model also increase with period as the work done by the system increase in the first 9 period units. But, efficiency of this model changes in a narrow range from 0.47 to 0.5. Even though, it is small range, it takes almost the same period interval to reach the quasistatic efficiency.

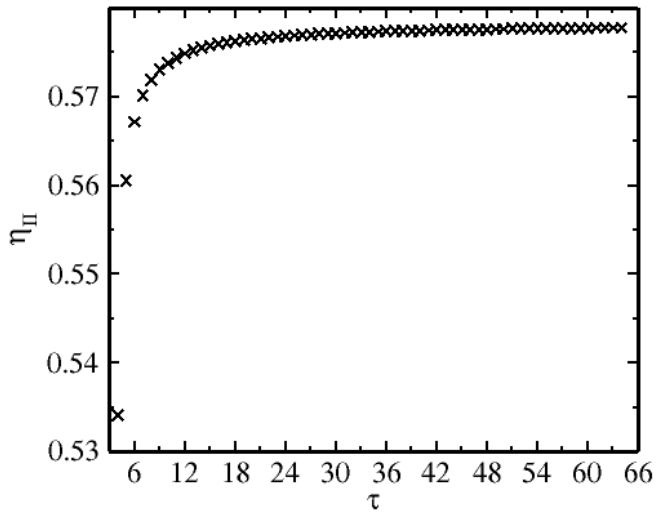

Figure 3.9: Plot of efficiency versus period for model II. $\beta_3 = -1.0, \beta_4 = -2.75, p^E = 0.64$ and $p^F = 0.74$..

In the next Chapter, we deal with optimized quantities: optimized period, optimized power and optimized efficiency of the model engines and their corresponding figure of merits.

Chapter 4

Optimized power, period and efficiency

In this Chapter we present the optimized power, period and efficiency of the models It is clear that optimization for energy transduction devices plays an important role in energy utilization as it improves efficiency. We optimize important quantities which are used to characterize how well the model engines perform in the optimum working conditions. Since maximum power working condition which accomplish a task in a very short time is costly energy-wise and quasistatic working condition is costly time-wise, engines' performance under optimized condition is another option to consier.

Optimizing thermodynamic quantity is finding the quantity of interest that leads to a process out of which as much work as possible is harvested while, at the same time, performing with efficiency better than that of efficiency at maximum power [23]. And also power-wise, it should give a non-zero finite power output contrary to the power of a quasistatic process. The aim of optimization is, therefore, to look for the rate at which the engine operates better both power-wise and efficiency-wise [23].

A number of optimization methods have been proposed by researchers, but as most of them lack generality, they are only applicable to specific heat devices [30, 31]. However, A.C. Hern*á*nadez *et.al* [23] have come up with a unified criterion for optimization of any energy converters. According to these authors, a thermodynamic criterion devoted to analyze the optimum regime of operation in a real process should meet three re-

quirements: its dependence on the parameter of the process should be a guide in order to improve the performance of the process; it should not depend on the parameter of the environment and finally, it should take into account the unavoidable dissipation of energy provoked by the process. It is used to identify the point of operation of an engine where the trade-off between energy cost and fast transport is compromised. The criterion, tested against a number of model engines, is found to qualify in a number of simple heat engines, for example, [21, 22, 24]. For irreversible heat engines, the criterion gives a performance of an optimized efficiency that is not as poor as the poor efficiency of a fast process(η_{mp}), nor as ideal as the maximum efficiency of a quasistatic process (η_q); it is found to lie somewhere between these extreme values - a regime considered optimum. Power-wise, the criterion gives a value which is not as poor as the power of a very slow (fast) nor as large as that of a maximum power, rather, it lies somewhere between the two values. For these reasons, we use this method to optimize thermodynamic quantities of our model heat engines.

The criteria used by A.C. Hernández *et.al* [23] are as follows. Suppose that for a given input energy $E_{in}(x;\{\gamma\})$ the heat engine produces a useful energy $E_u(x;\{\gamma\})$ per cycle, which is the difference between the maximum $E_{max}(\{\gamma\})$ and minimum $E_{min}(\{\gamma\})$ amount of energy that can be possibly extracted. $E_{min}(\{\gamma\})$ refers to the minimum possible amount of work that can be extracted from the engine under the worst condition while $E_{max}(\{\gamma\})$ refers to the maximum amount of work that can be extracted from the engine under a very slow speed and most efficient energy transduction. Thus the useful energy is in the range

$$E_{min}(\{\gamma\}) \leq E_u(x;\{\gamma\}) \leq E_{max}(\{\gamma\}), \tag{4.1}$$

where x is the independent parameter and $\{\gamma\}$ denotes a set of parameters similar to the external magnetic field which can be controlled. Here, we define two important quantities. The first is effective useful energy $E_{u,eff}(x;\{\gamma\})$, the difference between the useful energy and the minimum amount of energy that can be extracted from the engine, defined as

$$E_{u,eff}(x;\{\gamma\}) = E_u(x;\{\gamma\}) - E_{min}(\{\gamma\}), \tag{4.2}$$

and the second is the lost useful energy $E_{L,u}(x;\{\gamma\})$, the difference between $E_{max}(\{\gamma\})$

and useful energy

$$E_{L,u}(x;\{\gamma\}) = E_{max}(\{\gamma\}) - E_u(x;\{\gamma\}). \tag{4.3}$$

To evaluate the best compromise between useful energy and lost useful energy, an objective function (called Ω - function) is introduced [23] as the difference of these two quantities:

$$\Omega(x;\{\gamma\}) = E_{u,eff}(x;\{\gamma\}) - E_{L,u}(x;\{\gamma\}). \tag{4.4}$$

Note that in optimizing, the output energy should be as close as possible to the maximum output energy; the lost useful energy as small as possible in such a way that the useful output energy is as close as possible to the maximum output energy and as a result, the effective useful energy is large enough that the engine yields more work, see Fig. 4.1.

On the other hand, the efficiency of the engine is defined as the ratio between the useful energy $E_{u,eff}(x;\{\gamma\})$ and the input energy, $E_{in}(x;\{\gamma\})$:

$$\eta(x;\{\gamma\}) = \frac{E_{u,eff}(x;\{\gamma\})}{E_{in}(x;\{\gamma\})}. \tag{4.5}$$

$\eta(x;\{\gamma\})$ satisfies the condition

$$\eta_{min}(\{\gamma\}) \leq \eta(x;\{\gamma\}) \leq \eta_{max}(x;\{\gamma\}) \tag{4.6}$$

where $\eta_{min}(\{\gamma\})$ and $\eta_{max}(\{\gamma\})$ are the minimum and the maximum values of $\eta(x;\{\gamma\})$, respectively.

Fig. 4.1 illustrates the effective useful energy and the lost useful energy. The minimum output energy corresponds to the worst performance of the heat engine where it delivers the least work out of the input energy. The maximum output energy corresponds to the best performance of the heat engine where it delivers most of the input energy to work.

When the output energy is made close the maximum output energy, the effective useful energy increases thereby decreasing the amount of lost useful energy. On the other hand, when the output energy decreases and becomes closer to the minimum out put

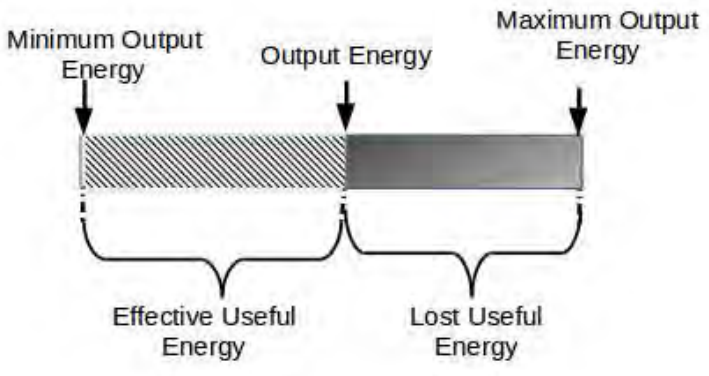

Figure 4.1: Schematic representation of the output energy by the heat engine under the worst, optimized and best conditions and ranges of Effective useful Energy and Lost useful Energy.

energy, the effective useful energy decreases. The former increases the efficiency of the heat engine whereas the latter decreases it. Somewhere in between the two would lead to optimized performance.

So far, we have been discussing quantities in general terms. At this point, let us use the independent parameter of our model, time t and leave the set of parameter $\{\gamma\}$ as it is. So the objective function, Eq.4.4, becomes

$$\Omega(t, \{\gamma\}) = (2\eta(t, \{\gamma\}) - (\eta_{max} + \eta_{min}))Q^f_{in}(t, \{\gamma\}). \tag{4.7}$$

We can further drop the set of control parameters in the sense that they will not explicitly be written in the expressions of the objective function. Our interest in this study is in the case where the minimum efficiency is zero and the maximum efficiency is η_C. The objective function per unit time is

$$\dot{\Omega}_I = (2\eta - \eta_q)\dot{Q}^f_{in}, \tag{4.8}$$

where Ω_I is the objective function of model I, $\eta_{max} = \eta_C$, $\eta_{min} = 0$, $\eta = \dot{Q}_{net}/\dot{Q}_{in}$ and $\dot{\Omega}$ denotes the objective function per unit time of model I.

4.1 Optimized period (τ_{opt}), optimized power(P_{opt}) and optimized efficiency (η_{opt}) of model I

To find the optimized quantities of model I, we should subject the objective function per unit time ($\dot{\Omega}_I(t)$) to the condition:

$$\frac{d\dot{\Omega}_I(t)}{dt}|_{t=\tau_{opt}} = 0, \tag{4.9}$$

and quest for τ_{opt}. The optimized power and efficiency can be computed from $P(\tau_{opt})$ and $\eta(\tau_{opt})$. τ_{opt} is the period at which the engine performs at optimum speed. The optimized period, τ_{opt} is

$$\tau_{opt} = 2(1 + \frac{1}{2}\eta_C z)\tau_{mp} \tag{4.10}$$

Thus, the corresponding optimized power, P_{opt}, becomes

$$P_{opt} = \frac{3}{4}\frac{(1 + \frac{2}{3}\eta_C z)}{(1 + \frac{1}{2}\eta_C z)^2}P_{mp}. \tag{4.11}$$

Using the value of τ_{opt} in Eq.(3.10), the optimized efficiency becomes

$$\eta_{opt} = \frac{3}{4}\frac{(1 + \frac{2}{3}\eta_C z)}{(1 + \frac{3}{4}\eta_C z)}\eta_C. \tag{4.12}$$

the expressions for K,L and P_{mp} are previously given in Sec.3.6.2.

4.1.1 P_{opt} and η_{opt} of model III

To find the optimized quantities of model III, we should subject its objective function per unit, $\dot{\Omega}_{III}(t)$, to the condition:

$$\frac{d\dot{\Omega}_{III}(t)}{dt}|_{t=\tau_{opt}} = 0, \tag{4.13}$$

where $\dot{\Omega}_{III}(t) = 2\dot{Q}_{net} - \eta_c\dot{Q}_{in}$ and search for τ_{opt}. The optimized power and efficiency can be computed from $P(\tau_{opt})$ and $\eta(\tau_{opt})$. τ_{opt} is the period at which the engine performs under optimum condition. Using eqs.(3.14) and (3.17), the optimized period, τ_{opt} is

$$\tau_{opt} = 2(1 + \frac{1}{2}\eta_q x)\tau_{mp}, \tag{4.14}$$

Thus the corresponding optimized power, $P_{opt} = P_{III}(\tau_{opt})$, becomes

$$P_{opt} = \frac{3}{4}\frac{(1 + \frac{2}{3}\eta_C x)}{(1 + \frac{1}{2}\eta_C x)^2}P_{mp}. \tag{4.15}$$

And the optimized efficiency, $\eta_{opt} = \eta(\tau_{opt})$, of the model is

$$\eta_{opt} = \frac{3}{4}\frac{(1 + \frac{2}{3}\eta_C x)}{(1 + \frac{1}{4}\eta_C x)}\eta_C. \tag{4.16}$$

The expression of x in Eqs. 4.15- 4.16 is $K^{'}/L'$, see Sec.3.4.6. Whereas the expression for P_{mp} is given in Eq. 3.50.

4.1.2 P_{opt} and η_{opt} of model II

To find the optimized quantities of model II, similar to models I and III, we should subject its objective function per unit, $\dot{\Omega}_{II}(t)$, to the condition:

$$\frac{d\dot{\Omega}_{II}(t)}{dt}|_{t=\tau_{opt}} = 0, \tag{4.17}$$

where $\dot{\Omega}_{II}(t) = 2\dot{Q}_{net} - \eta_c\dot{Q}_{in}$ and search for τ_{opt} for the model. The optimized power and efficiency can be computed from $P(\tau_{opt})$ and $\eta(\tau_{opt})$. τ_{opt} is the period at which the engine performs under optimum condition. Using eqs.(3.14) and (3.17), the optimized period, τ_{opt} is

$$\tau_{opt} = 2(1 - \frac{1}{2}\eta_q \chi)\tau_{mp}, \tag{4.18}$$

Thus the corresponding optimized power, $P_{opt} = P_{II}(\tau_{opt})$, becomes

$$P_{opt} = \frac{3}{4}\frac{(1 - \frac{2}{3}\eta_C \chi)}{(1 - \frac{1}{2}\eta_C \chi)^2}P_{mp}. \tag{4.19}$$

And the optimized efficiency, $\eta_{opt} = \eta(\tau_{opt})$, of the model is

$$\eta_{opt} = \frac{3}{4}\frac{(1 - \frac{2}{3}\eta_C \chi)}{(1 - \frac{3}{4}\eta_C \chi)}\eta_C. \tag{4.20}$$

The expression of χ in Eqs. 4.18- 4.20 is v/V, see sec.3.5.6. Whereas the expression for P_{mp} is given in Sec. 3.6.2.

4.2 The figure of merit ψ

The other most important quantity to analyze such a heat engine is the figure of merit. The figure of merit ψ is a quantity used to characterize the overall performance of a device. Previously, it has been defined for a thermoelectric single-level quantum dot as a the ratio of the product of scaled quantities of power and efficiency to period,[21]. However, we realize that the contribution of period has been two fold: one from period itself and the other from power. So, to avoid double count in period, we drop the contribution of period in the calculation of the figure of merit and redefine it as as the product of scaled power ω and scaled efficiency ϵ. Scaled quantity, in our context, is the ratio of the optimized quantity to the quantity at maximum power. Hence, the scaled power ω, the scaled efficiency ϵ and the the figure of merit ψ are, respectively, defined as follows. The scaled power for model I, ω_I, is

$$\omega_I = \frac{P_{opt}(I)}{P_{mp}(I)}. \tag{4.21}$$

The scaled power for model III, ω_{III}, is defined as

$$\omega_{III} = \frac{P_{opt}(III)}{P_{mp}(III)}. \tag{4.22}$$

The scaled power for model II, ω_{II}, is defined as

$$\omega_{II} = \frac{P_{opt}(II)}{P_{mp}(II)}. \tag{4.23}$$

The scaled efficiencies for models I, III and II, respectively, are

$$\epsilon_I = \frac{\eta_{opt}(I)}{\eta_{mp}(I)}, \quad \epsilon_{III} = \frac{\eta_{opt}(III)}{\eta^*_{mp}(III)}, and \quad \epsilon_{II} = \frac{\eta_{opt}(II)}{\eta^*_{mp}(II)} \tag{4.24}$$

where $\eta^*_{mp}(III)$ and $\eta^*_{mp}(II)$ are, respectively, the particular efficiency values at the maximum power of models III and II.

$$\omega_I = \frac{3}{4}\frac{(1+\frac{2}{3}\eta_C z)}{(1+\frac{1}{2}\eta_C z)^2}, \quad \omega_{III} = \frac{3}{4}\frac{(1+\frac{2}{3}\eta_C x)}{(1+\frac{1}{2}\eta_C x)^2} \tag{4.25}$$

$$\epsilon_I = \frac{3}{2}\frac{(1+\frac{2}{3}\eta_C z)(1+\frac{1}{2}\eta_C z)}{(1+\frac{3}{4}\eta_C z)\eta^*_{mp}(I)}, \quad \epsilon_{III} = \frac{3}{4}\frac{(1+\frac{2}{3}\eta_C x)}{(1+\frac{1}{4}\eta_C x)\eta^*_{mp}(III)} \tag{4.26}$$

The expression for scaled power, ω_{II}, and scaled efficiency, ϵ_{II}, for model II, are

$$\omega_{II} = \frac{3}{4}\frac{(1-\frac{2}{3}\eta_C\chi)}{(1-\frac{1}{2}\eta_C\chi)^2}, \quad \epsilon_{II} = \frac{3}{4}\frac{(1-\frac{2}{3}\eta_C\chi)}{(1-\frac{3}{4}\eta_C\chi)\eta_{mp}(II)} \tag{4.27}$$

The figure of merit ψ_I for model I, which is the product of ω_I and ϵ_I becomes

$$\psi_I = \frac{9}{16}\frac{(1+\frac{2}{3}\eta_C z)^2}{(1+\frac{1}{2}\eta_C z)(1+\frac{3}{4}\eta_C z)\eta^*_{mp}(I)}. \tag{4.28}$$

The figure of merits ψ_{III} and ψ_{II} for models III and II, the product of their respective which is the ω and ϵ become

$$\psi_{III} = \frac{9}{16}\frac{(1+\frac{2}{3}\eta_C x)^2}{(1+\frac{1}{2}\eta_C x)^2}((1+\frac{1}{4}\eta_C x)\eta^*_{mp}(III))^{-1}. \tag{4.29}$$

$$\psi_{II} = \frac{9}{8}\frac{(1-\frac{2}{3}\eta_C\chi)^2}{(1-\frac{1}{2}\eta_C\chi)^2}((1-\frac{3}{4}\eta_C\chi)((1-0.5\chi\eta_C))(II))^{-1}. \tag{4.30}$$

In this Chapter, we have proposed three theoretical model engines two of which operate between two reservoirs at positive inverse temperatures and a third one that operate between two negative absolute temperatures at finite-time schemes. The finite-time thermodynamic processes are described and the expressions of the accompanying quantities are derived . The engine's performance is explored under optimized working conditions. The optimum point of operation for the engines is determined. From the estimation of the figure of merit suggested for the models, better performances are found under the engine's optimized operation than that of the maximum power working conditions.

4.3 Results and Discussion

In this subsection, the comparisons between the optimized power and efficiency with their values at maximum power for the models are plotted against the quasistatic efficiency.

4.3.1 Scaled power, scaled efficiency and figure of merit for model I

Here, we compare the optimized power with the maximum power and optimized efficiency with efficiency at the maximum power of model I. The left parts of Eqs.4.27 and 4.25, respectively, have been derived for scaled optimized efficiency and scaled optimized power for the model. So, using these equations, we plot and discuss scaled optimized power, scaled efficiency and the figure of merit against the quasistatic efficiency.

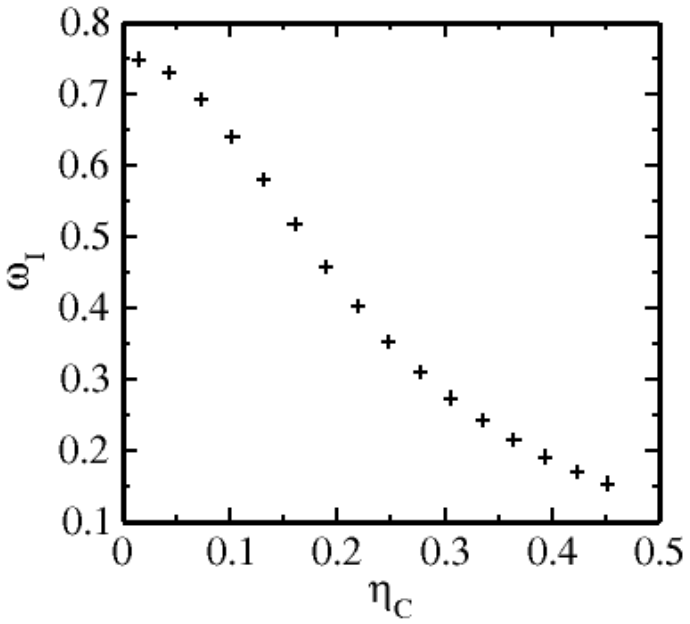

Figure 4.2: Plot of scaled power ω_I versus η_q for model I. $\beta_1 = 0.80, \beta_2 = 1.5, p^A = 0.02$ and $p^B = 0.34$.

Fig.4.2 shows a plot of scaled power, ω_I, versus quasistatic efficiency, η_C for model I. As the quasistatic efficiency(η_C) increases, scaled power decreases. As the plot clearly shows, the engine utilizes a maximum of 75% of the maximum available power at a very small values of η_C. When the quasistatic efficiency increases from zero to three-fourth of the maximum possible value, the scaled power has lost about 70% of its maximum power. Eventually, at the maximum value of η_C, the engine is performing with a value quite less than 20% of the peak scaled power.

Fig.4.3 is a plot of the scaled efficiency, ϵ_I, versus the quasistatic efficiency, η_C for model

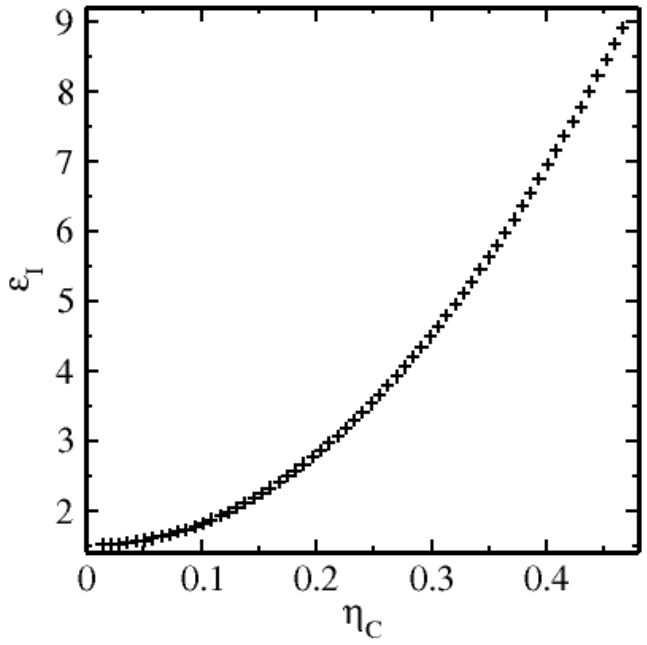

Figure 4.3: Scaled optimized efficiency, ϵ_I versus η_C. $\beta_1 = 0.80, \beta_2 = 1.5, p^A = 0.02$ and $p^B = 0.34$.

I. As the quasistatic efficiency increases from zero to the maximum possible η_q value, ϵ_I increases monotonically from about 1.5 to a maximum of 9. The increment of ϵ_I, the ratio of two efficiencies, is due to two reasons. The first one is the net work done by the system increase with time. The second is efficiency at maximum power, the denominator of the expression for ϵ_I, deceases with time. The combination of these makes ϵ_I gains a factor of about 6 folds in the quasistatic limit. So, efficiency-wise the optimum working condition has a better advantage than the maximum power working condition.

Fig. 4.4 is a plot of the figure of merit, ψ_1, versus quasistatic efficiency, η_C for model I. Figure of merit is a product of scaled power and scaled efficiency. It is, therefore, a compromise between the decreasing scaled power and the increasing scaled efficiency of the model. Except in the region $0.05 < \eta_C < 0.25$, where ψ_1 is relatively rising, it is observed that the figure of merit is steadily increasing with increase in η_C. In particular, when η_C close to zero, ψ_I is very slowly increasing with η_C. Whereas as η_C approaches its maximum value of 0.46, ψ_I, the increasing scaled efficiency and the decreasing scaled power tends to balance each other.

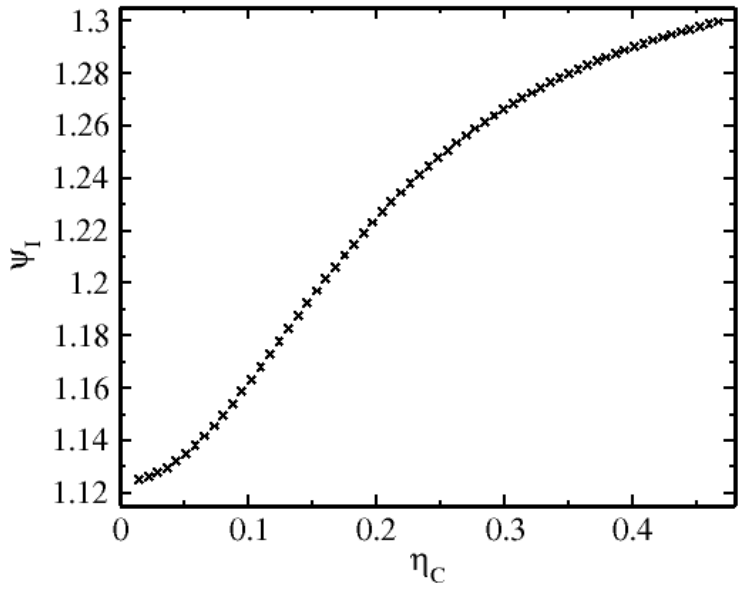

Figure 4.4: Plot of figure of merit versus η_C. $\beta_1 = 0.80, \beta_2 = 1.5, p^A = 0.02$ and $p^B = 0.34$.

4.3.2 Scaled power, scaled efficiency and figure of merit for model III

In this subsection, the comparisons between the optimized power and efficiency with their values at maximum power for model III are plotted against the quasistatic efficiency. We employ the right part of Eqs.(4.19), (4.20) and (4.21) for the plots.

Fig.4.5 shows a plot of scaled power (ω_{III}) versus quasistatic efficiency, η_C for model III. In this model also as the quasistatic efficiency(η_C) increases, scaled power decreases in a similar trend to that of ω_I. As we observe in Fig.5.10, the engine utilizes a maximum of about 75% of the maximum available power at a very small values of η_C. When the quasistatic efficiency(η_C) increases from zero to three-fourth of the maximum possible quasistatic value, the scaled power has already lost about 90% of its maximum power. Eventually, at the maximum value of η_C, the engine is performing with only 5% of the peak power. The comparison between ω_I and ω_{III} shows $\omega_I > \omega_{III}$ in the ranges of values where they can be compared, see inset of Fig.5.10. The inset shows that in the entire range of possible η_C, model I is more powerful than model III.

Fig.4.6 is a plot of the scaled efficiency ϵ_{III} versus the quasistatic efficiency, η_C, for

Figure 4.5: Plot of scaled power ω_{III} versus η_q. $\beta_5 = 0.5, \beta_6 = 1.5, p^d = 0.54$ and $p^c = 0.8$. Inset is the comparison between ω_I and ω_{III}. Note that the condition under which model I performs is different from model III.

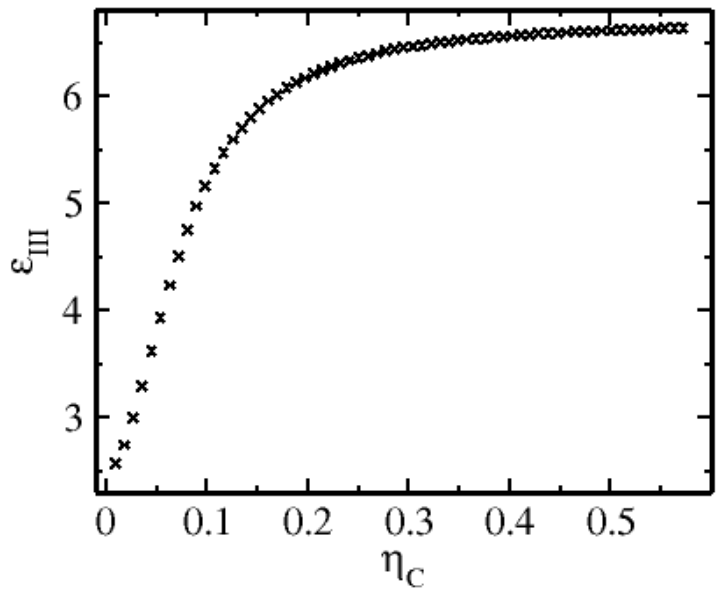

Figure 4.6: Plot of scaled efficiency ϵ_{III} versus η_q. $\beta_5 = 0.50$, $\beta_6 = 1.5$, $p^d = 0.54$ and $p^c = 0.80$.

model III. In the very smallη_C values (from 0 to 0.2), ϵ_{III} increases almost exponentially from about 6. The fact that efficiency increase with an increase in the net heat absorbed has contributed to the gain in efficiency. We observe a steady increase in scaled efficiency as the quasistatic efficiency increases beyond 0.2 and finally leveled off. So, efficiency-wise the optimum working condition has a better advantage over the maximum power working condition.

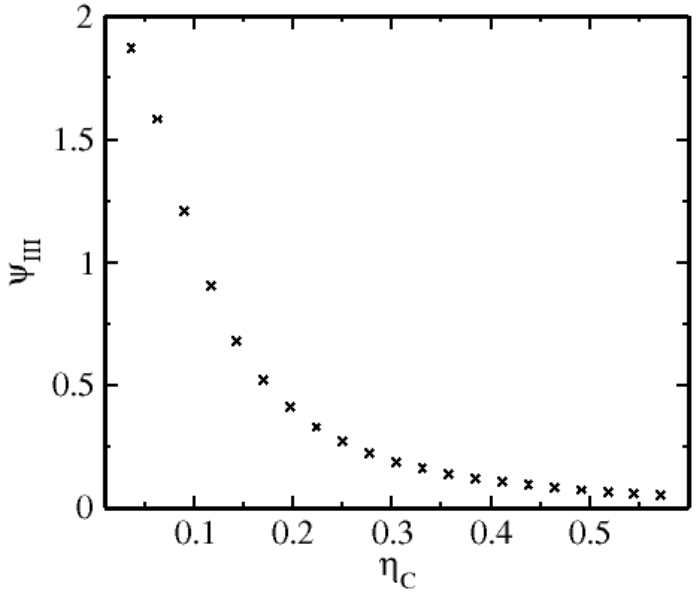

Figure 4.7: Plot of figure of merit versus η_q for model III. $\beta_5 = 0.50$, $\beta_6 = 1.5$, $p^d = 0.54$ and $p^c = 0.80$.

Fig.4.7 depicts the figure of merit ψ_{III} versus η_C for model III. The figure of merit ψ_{III} for this model, the product of scaled power ω_{III} and scaled efficiency ϵ_{III}, tells us how well the system is performing as compared to its value at the maximum power. ψ_{III} is about 1.89 as $\eta_C \to 0$. The figure of merit for the model drops sharply as the η_C increases. One can easily observe from the plot how the scaled power dominates the scaled efficiency for the model. The plot also shows mixed advantages: In the case where $0 < \eta_C < 0.1$, $\psi_{III} > 1$ and hence optimum working condition is referred to the maximum power working condition. However, when $\eta_C > 0.1$, $\psi_{III} < 1$ and, therefore, maximum working condition is preferable to the optimum condition.

Figure 4.8: Plots of ω_{II}, ϵ_{II} and ψ_{II} versus η_C for model II. $\beta_3 = -1.0$, $\beta_4 = -2.75$, $p^E = 0.64$ and $p^F = 0.74$.

Fig. 4.8 shows the scaled power(upright triangle), scaled efficiency(plus sign) and figure of merit(cross) versus η_C for model II. The scaled power, ω increases linearly from 0.75 to about 0.94. Since the optimized power of the model engine is scaled with its maximum power, it is expected that ω of the model should remain less than unity in the entire range of η_C. The scaled efficiency of the model ϵ, however, decreases linearly from 1.47 to about 1.1 as η_C increases. The figure of merit, ψ_{II}, also decreases from its peak value of 1.1209 to about 1.04, but no appreciable change is observed in ψ_{II} as compared to the scaled power and scaled efficiency. $\psi_{II} > 1$ and that the optimized mode of operation is better than its maximum mode of operation for the model.

Chapter 5

Summary and Conclusion

In this Chapter we summarize and give brief conclusion to the findings of our work. In the present work, we model engines which perform tasks due to interaction between thermal reservoirs and time dependent external magnetic field. A system of spin-half particles is taken as a working substance between two reservoirs where the reservoirs are either at two distinct positive or negative absolute temperatures. The systems are studied in the quasistatic and finite-time schemes and relevant thermodynamic quantities are derived.

Room temperature of 300 K and k_BT are, respectively, chosen to scale temperature and energy; all values and numerical figures presented in this work are given in terms of these units. In the Finite-time processes simple Fortran Programmings are used to generated data to plot quantities; however, the data are rounded off to two decimal point for simplicity.

A complete cycle in the quasistatic processes consists slowly changing isothermal processes where the system and the reservoirs are in thermal equilibrium and fast changing adiabatic processes which link the isothermal processes. In the slowly changing isothermal processes there are work done by(on) the system and heat exchange between the system and the reservoirs. In the adiabatic processes, there are only work done by(on) the system. From the net heat absorbed by the system, efficiency, perhaps the most important quantity in the discussion of the quasistatic process is derived analytically for the three models to help compare with the corresponding finite-time processes.

A complete cycle in the finite-time process is a combination of alternate adiabatic change, relaxation of the system at constant external field and a (thermalization) process that takes place at constant external magnetic filed so as to allow thermal interactions. The finite-time process is systematically adapted from the quasistatic process in such a fashion that the system is adiabatically detached from a reservoir then relax to a new equilibrium and attached to a reservoir until the system equilibrate with the reservoir and detach and so on. So, it follows a series of three distinct basic blocks in a complete cycle. As compared to the quasistatic process, this is faster and represents real process. From the changes in the occupation probability in the excited state and the energy level spacings, net heat absorbed, power and efficiency for each models are determined.

For the finite-time models, the plots of power versus period of the three models are found to be monotonically increasing when time of operation is small but not too small. Power attains a maximum value, P_{mp} at some finite-time τ_{mp} and then decline for further increase in period. when period is longer and longer, power keeps decreasing and eventually approaches the small quasistatic limit.

Period at maximum power is shorter than the optimized period in the three models; hence period-wise, the engines accomplish a task in a shorter period of time under its maximum power working conditions. But, efficiencies at the maximum power are poorer than the respective optimized efficiencies. So, efficiency-wise, maximum power working conditions do not have advantage. Due to this fact, operation under the optimized condition is explored for the models.
We employed an optimization criterion suggested by A.C. Hernández *it.al* [23] to optimize and compared the optimized values to the corresponding quantities at the maximum power. According to the comparisons made for model I and III, the optimized power is about three-fourth of the maximum power when the quasistatic efficiency of the models is very small($\eta_C \to 0$) and decline for higher quasistatic efficiency values. So, the engines are powerful when η_q is small. For model II, however, the optimized power increases as the quasistatic efficiency of the models increases from zero to its maximum value, $\eta_C = 0.63$.

Each optimized periods is found to be at least twice the period of the maximum power for each model, see Eqs. (4.10) and (4.14). The optimized efficiency of models I is at least one and half times the efficiencies at the maximum power and increases monotonically for further increase in quasistatic efficiency. A gain of about six fold is observed in the scaled efficiency for model I. Scaled with respect to the efficiency at the maximum power, the optimized efficiency of model III is at most 1.89 time the efficiency of the model at maximum power and decreases as the quasistatic efficiency of the models increase. It takes longer period for each system when they perform under optimized conditions than under the maximum power. It can be possible to conclude that from efficiency point of view, each models utilize more energy under the optimized conditions than the maximum power condition but at the expense of longer periods. The scaled efficiency of model II, ϵ, decreases from 1.47 to about 1.1 as η_C increases. To compare the advantages of the engines, we introduce the figure of merit,ψ to each model and quantify the overall performance of the models under study. The scaled power, ω and scaled efficiency, ϵ with respect to their values at maximum power are used in the estimation of the performance of the engines. Hence, the figure of merit of the heat engine is defined as the product of the scaled quantities. In model I, the figure of merit increases as the η_C increases; but for models II and III, the figure of merit decreases. Note that $\psi > 1$ would mean that the performance of the system is better under the optimized condition than under the maximum power mode of operation. So, in the entire range of quasistatic efficiency, the model engines proposed have good ψ.

The scaled power, ω increases linearly from 0.75 to about 0.94. Since the optimized power of the model engine is scaled with its maximum power, it is expected that ω of the model should remain less than unity in the entire range of η_C. The scaled efficiency of the model ϵ, however, decreases linearly from 1.47 to about 1.1 as η_C increases. The figure of merit, ψ_{II}, also decreases from its peak value of 1.1209 to about 1.04, but no appreciable change is observed in ψ_{II} as compared to the scaled power and scaled efficiency. $\psi_{II} > 1$ and that the optimized mode of operation is better than its maximum mode of operation for the model.

Bibliography

[1] C.Tsallis and L.J.L Cirto, Eur. Phys. J. Special Topics,**223**, 2162 (2014).

[2] H.B. Callen, *Thermodynamics and an Introduction to Thermostatistics*, John Wiley and Sons, 2nd Edn (1985).

[3] K. Huang, *Statistical Mechanics*, Wiley, 2nd Edn (1987).

[4] S.R.A Salinas, *Introduction to Statistical Physics*, Springer (2001).

[5] M. Toda, R. Kubo and N.Sait$\widehat{o}$, *Statistical Physics I*, Sringer-Verleg, (1983).

[6] S. Braun, J. P. Ronzheimer, M, Schreiber, S.S. Hodgman, T. Rom, I. Bloch and U. Schneider, Science **339**,52 (2013).

[7] C. Luca, A. Puglis and A. Vulpiani, IOP, **41**, xxx (2015).

[8] E. M. Purcell and R.V. Pound, Phys. Rev., **81**, 279 (1951).

[9] F. N. Ramsey, Phys. Rev., **103**, 20 (1956).

[10] P. T. Landsberg, Phys. Rev., **115**, 518 (1959).

[11] S. Braun and U. Schneider, *Negative Absolute Temperature*, *http://www.quantum-munich.de/research/negative-absolute-temperature/*

[12] R. K. Pathria and P.D. Beale, *Statistical Mechanics*, Elsevier, 2nd Edn (1996).

[13] Z. C. TU, J. Phys. A: Math. Theor., **41**, 312003(2008).

[14] F. L. Curzon and B. Ahlborn, Am. J. Phys., **43**, 22 (1975).

[15] S. Hilbert, P. Hanggi and J. Dunkel, Phys. Rev. E **90**, 1408 (2014).

[16] D. Frenkel and P. B. Warren,Am. J. Phys., **83**, 163 (2015).

[17] H. T. Quan., S. Yang and C. P. Sun, Phys. Rev. E **78**, 021116 (2008).

[18] E. Geva and R. Kosloff, J. Chem. Phys., **97**, 4398 (1992).

[19] A. Jacques, L. Chusseau and F. Philippe, arXiv:quant-ph/0211072v2 (2008).

[20] D. T. Kieu, Phys. Rev. Lett. **93**, 140403(2004).

[21] F. Borga, M. Bekele, T. Yourgu and M. Tsige, Phys. Rev. E **86**, 032106 (2012).

[22] M. Asfaw and M. Bekele, Eur. Phys. B **38**, 457(2004).

[23] A. C. Hernánadez, A. Medina, J. M. M. Roco, A. J. White and S. Velasco, Phys. Rev. E **63**, 037102 (2001).

[24] Sánchez-Salas, L. López-Palacio, S. Velasco, and A. C. Hernández, Phys. Rev. **E** 82, 051101(2010)

[25] M. Alemye, Efficiency, power and period of a model quantum heat engine working in a finite time, AAU, Unpublished M. Sc. Thesis (2011).

[26] W. Chegeno, The efficiency of a simple quantum heat engine, AAU, Unpublished M. Sc. Thesis (2011).

[27] H. T Odum and R. C. Pinkerton, Amer. Sci, **43**, 331 (1955).

[28] M. Esposito, K. Lindenberg and C. Van den Broeck, Phys. Rev. Lett., **102**, 130602 (2009).

[29] A. Gomez-Marin and J. M. Sancho, Phys. Rev. E **74**, 214 (2006).

[30] R. S. Berry, V. A. Kazakov, S. Sieniutycz, Z. Szwast and A. M. Tsirling, *Thermodynamic Optimization of Finite-Time Processes*, Wiley (2000).

[31] C. Wu, L. Chen and J. Chen, *Recent Advances in Finite Time Thermodynamics*, nova Science (1999).